

Alma Mater Studiorum Università di Bologna
Archivio istituzionale della ricerca

River avulsions and sedimentary evolution of the Luanhe fan-delta system (North China) since the late Pleistocene

This is the final peer-reviewed author's accepted manuscript (postprint) of the following publication:

Published Version:

He, L., Amorosi, A., Ye, S., Xue, C., Yang, S., Laws, E.A. (2020). River avulsions and sedimentary evolution of the Luanhe fan-delta system (North China) since the late Pleistocene. MARINE GEOLOGY, 425, 106194-106214 [10.1016/j.margeo.2020.106194].

Availability:

This version is available at: <https://hdl.handle.net/11585/871218> since: 2023-04-12

Published:

DOI: <http://doi.org/10.1016/j.margeo.2020.106194>

Terms of use:

Some rights reserved. The terms and conditions for the reuse of this version of the manuscript are specified in the publishing policy. For all terms of use and more information see the publisher's website.

This item was downloaded from IRIS Università di Bologna (<https://cris.unibo.it/>).
When citing, please refer to the published version.

(Article begins on next page)

This is the final peer-reviewed accepted manuscript of:

He L.; Amorosi A.; Ye S.; Xue C.; Yang S.; Laws E.A.: *River avulsions and sedimentary evolution of the Luanhe fan-delta system (North China) since the late Pleistocene*

MARINE GEOLOGY VOL 425 ISSN: 0025-3227

DOI: 10.1016/j.margeo.2020.106194

The final published version is available online at:

<https://dx.doi.org/10.1016/j.margeo.2020.106194>

Terms of use:

Some rights reserved. The terms and conditions for the reuse of this version of the manuscript are specified in the publishing policy. For all terms of use and more information see the publisher's website.

This item was downloaded from IRIS Università di Bologna (<https://cris.unibo.it/>)

When citing, please refer to the published version.

River avulsions and sedimentary evolution of the Luanhe fan-delta system (North China) since the Late Pleistocene

Lei He ^{a, b}, Alessandro Amorosi ^c, Siyuan Ye ^{a, b*}, Chunting Xue ^a, Shixiong Yang ^{a, b}

^a Key Laboratory of Coastal Wetland Biogeosciences, Qingdao Institute of Marine Geology, China Geologic Survey, Qingdao, 266071, China

^b Laboratory for Marine Geology, Qingdao National Laboratory for Marine Science and Technology, Qingdao, 266061, China

^c Department of Biological, Geological and Environmental Sciences, University of Bologna, Bologna, 40134, Italy

Abstract: The Luanhe Fan-Delta (LFD) is one of the most important coastal deltas in North China. Investigations on the late Quaternary evolution of this fan-delta system have been implemented significantly in the 1980s. However, detailed sedimentologic studies have seldom been undertaken. Based on the comprehensive analysis of sedimentary facies, grain size, microfossils, radiocarbon dates (AMS¹⁴C) and optically stimulated luminescence (OSL) ages from three ~30 m-long cores (BXZK01~03), along with recent reports from a series of cores and seismic profiles from the coastal areas, we reconstructed the detailed late Quaternary sedimentary evolution of the northern Bohai coast, which evolved from a coastal barrier-lagoon system during MIS5 to an alluvial plain, with river channels and floodplains between MIS4 and the Early Holocene. A variety of transgressive coastal depositional environments (freshwater marsh, sandy barrier, shallow sea) developed during the early Holocene, and followed by wave-dominated delta progradation (prodelta, coastal barrier and lagoon). Two dramatic 90-degree diversions of the lower Luanhe River course likely influenced the sedimentary evolution of LFD in its inner portion. The first avulsion took place in Qianxi, probably at the end of the Late Pleistocene (~15000 cal a BP). It led to the abandonment of the Luanhe alluvial fan in the western part of the northern Bohai coastal

plain (NBCP), and to the formation of a new alluvial fan in the eastern NBCP. This alluvial fan evolved into a fan-delta system (7000–3500 cal a BP) during the Holocene transgression. The second avulsion occurred at Zhuacun during the Late Holocene, probably at 3600 ±100 cal a BP. Following this latter avulsion, the Luanhe River shifted toward the east and formed a new fan-delta system (3700 cal a BP–present), with its apex in Luanzhou. Abrupt tectonic uplift in this highly seismic region likely controlled the two avulsions and the dramatic shift of alluvial-fan complexes. Climate and sea-level changes may also have partly influenced the development of LFD.

Keywords: Fan-delta, coastal barrier-lagoon system, river avulsion, sedimentary evolution, Luanhe River

*Corresponding Author: siyuanye@hotmail.com (S. Ye)

1. Introduction

Fan-deltas form where mountain streams build directly into lakes or shallow seas after exiting from narrow outlets, and show a variable degree of peripheral modification by basin hydrodynamics (Galloway and Hobday, 1983). A wide variety of fan-delta systems occurs as a function of transport dynamics (rivers, waves and tide currents), sediment supply, and morphology of the receiving basin (Coleman and Wright, 1975; Orton and Reading, 1993). These systems have attracted geologists' attentions for decades, as they (i) widely spread at the margins of modern and ancient basins in different tectonic settings (McPherson et al., 1988; Benvenuti, 2003; Lonne and Nemec, 2010; Jia et al., 2016), (ii) are good records of past changes in climate, sea/lake level and tectonic movements (Nava-Sanchez et al., 1999; Lopez-Blanco et al., 2000; Winsemann et al., 2007), and (iii) commonly contain vast hydrocarbon reservoirs (Wei et al., 2015; Jia et al., 2017). Several studies have documented in detail the stratigraphy, facies associations, and sedimentary evolution of fan-deltas developed in different tectonic settings, based on outcrops and subsurface data (Hwang et al., 1995; Dorsey et al., 1995; Kim and Chough, 2000; Rohais et al., 2008; Park et al., 2013).

The Luanhe Fan-Delta (LFD) is a popular coastal system in China. Previous studies on the Luanhe Delta in the 1980s mainly focused on the late Quaternary stratigraphy, modern depositional processes, and its spatial-temporal evolution (e.g. Gao, 1981, 1985; Li C. et al., 1982, 1983, 1984, 1985; Li Y. et al., 1982; GIDPF et al., 1985). However, due to paucity of subsurface (core) data and poor chronologic

control, a knowledge gap of Luanhe fan-delta evolution still exists, especially about the Holocene sedimentary evolution of the lower Luanhe Plain and its relationship with the upper Luanhe alluvial fan. Based on core facies analysis, stratigraphy and relatively precise ages from three ~30 m-long cores recovered in the Lower Luanhe Plain (LLP) in 2016 (Fig. 1), as well as using recent stratigraphic data from boreholes and seismic profiles around the present coastline, the aims of this paper are: (i) to reconstruct the detailed stratigraphic architecture of LFD, (ii) to examine its late Quaternary evolution, and (iii) to assess controlling factors on the sedimentary evolution of the LFD.

2. Geological background

2.1. The Luanhe River system and its landscape

The Luanhe River originates from Mountain Bayan Tugur in Hebei Province (North China), and flows across the Mongolia Plateau and the Yanshan Mountains (Fig. 1a). It leaves the Yanshan uplifted zone in Luanzhou after taking over the Qinglong River nearby, and empties into Bohai Sea in the Laoting area (Fig. 1b). The full river length is 877 km, and the total basin area is 44,900 km² (Feng and Zhang, 1998). The area consists predominantly of mountains and hills (98.2%), while LLP accounts for just 1.8% (Liu, 2012). The proportion of mountain-hill areas in the Luanhe River drainage is the largest among major rivers of Eastern China (Xue, 2016).

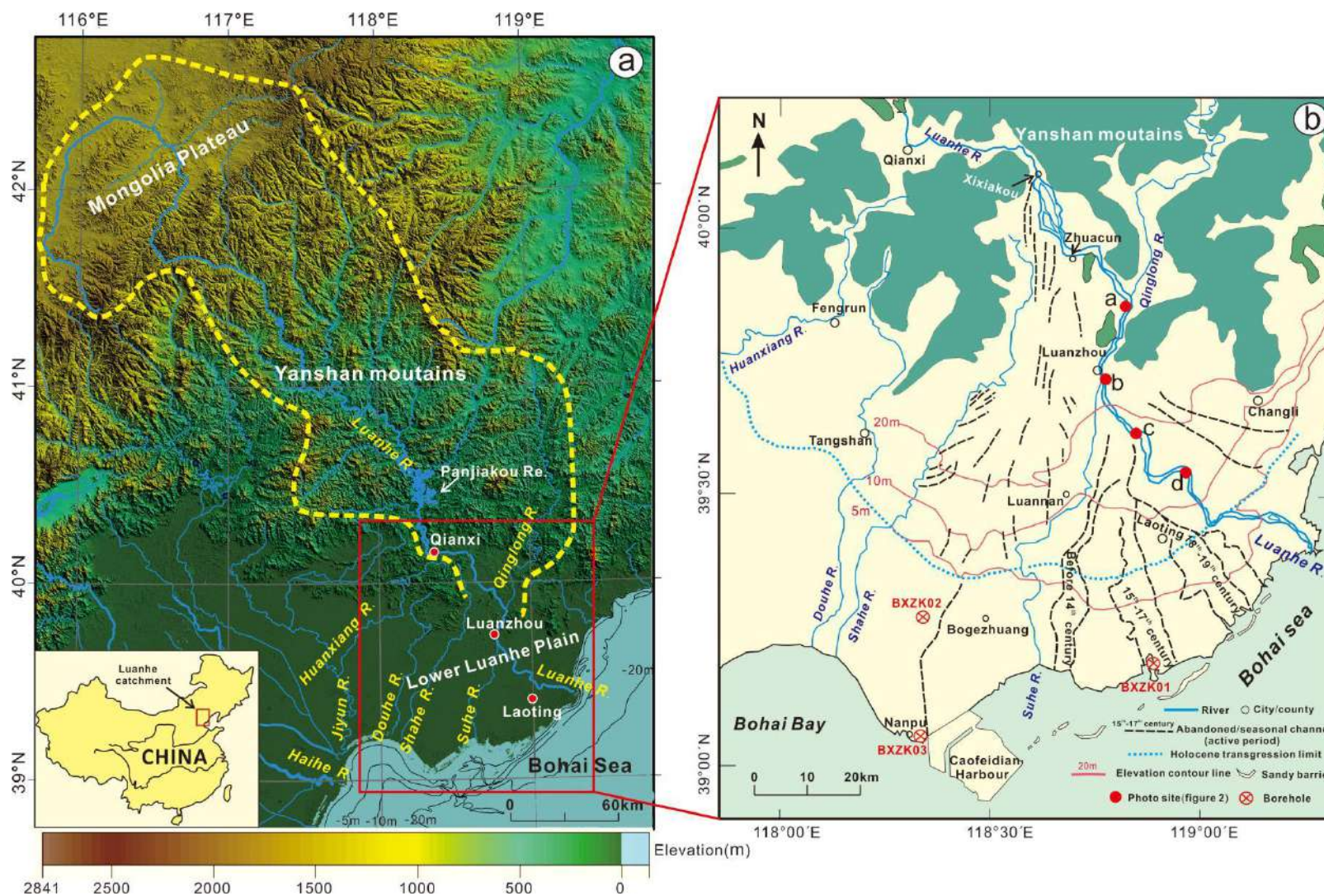


Fig.1 Geomorphology of the Luanhe drainage basin and distribution of drilling boreholes
in the Luanhe Fan-delta (LFD)

(a) The Luanhe River originates from the Mongolia Plateau, and flows across the Yanshan Mountains and the Lower Luanhe Plain (LLP), then finally discharges into the Bohai Sea. The DEM dataset was provided by Geospatial Data Cloud site, Chinese Academy of Sciences (<http://www.gscloud.cn>); (b) Present river channels and abandoned/seasonal courses in the LLP. Abandoned/seasonal courses are modified from [Gao \(1981\)](#) and [Mo \(1987\)](#). The landward limit of the Holocene transgression and contour lines are modified from [Xue \(2016\)](#).

The Luanhe River has high runoff and sediment discharge. Taking the storage time (1979) of the Panjiakou reservoir as a node ([Fig. 1a](#)), the average annual runoff of the river was $4.72 \times 10^9 \text{ m}^3$ from 1929 to 1979 under relatively pristine conditions, while the average annual sediment discharge was $22.19 \times 10^6 \text{ t}$ during the same period ([Guo and Fan, 1989](#)). Water and sediment discharges decreased dramatically after the storage in the Panjiakou reservoir and the construction of the Luanhe-Tianjin aqueduct (1983) ([Guo and Fan, 1989](#); [Li and Yin, 2010](#)). Based on data from [Li and Yin \(2010\)](#), annual water and sediment discharges during 1980–2003 were calculated to be only $1.17 \times 10^9 \text{ m}^3$ and $1.74 \times 10^6 \text{ t}$, respectively.

The sediment carried by the Luanhe River mainly derives from the Yanshan Mountains in the midstream, where ancient metamorphic rocks and different types of volcanic rocks are widely exposed ([Gao, 1985](#)). An arid continental climate and low vegetation coverage result in significant soil loss in this area, where the erosion modulus has been estimated to be up to 1440 t/km^2 ([Gao, 1985](#)). Water and sediment concentrate in the summer season, due to catchment characteristics and climate regime. A total of 68.4% water discharge concentrates during the flood season, from June to September. The Luanhe River also transports 99.3% of the total annual sediment load into the Bohai Sea from June to August ([Jiang et al., 1986](#)).

Four major river terraces (T1–T4) have been identified along the Luanhe River valley, north of Qianxi (Gao, 1987). Only two terraces (T1–T2) can be observed in the lower Luanhe River segment between Qianxi and Zhuacun (Fig. 1b), and just one terrace (T1) develops along the lower river bank south of Zhuacun (Gao, 1985, 1987). The Luanhe river channel is filled with gravel and coarse sand upstream of Luanzhou (Fig. 2a). The gravel content decreases sharply south of Luanzhou and the average grain size of channel-filled sediments also gradually decreases from the upstream region to the river mouth (Fig. 2b–2d). Sediment is silty sand and fine sand at the modern Luanhe River mouth (Li et al., 1985; Feng and Zhang, 1998).

Abandoned channels are widely distributed between Tangshan in the west and Luanzhou in the east (Fig. 1b). These channels are mostly considered as ancient Luanhe River courses of Holocene age that were fragmentarily incorporated in the landscape due to intense human activities (Mo, 1987). At least two buried sandy channel belts can be observed in the Changli area (Fig. 1b). Heavy mineral analysis revealed that these sediment bodies are fluvial sands assigned to an ancient Luanhe River course (Li et al., 1985). Seasonal stream courses prevail in the area between Luannan and Laoting (Fig. 1b). According to historical documents and aerial photographs, these rivers were active from the late 13th century to the late 19th century, representing main routes for the Luanhe River entering the Bohai Sea at that time (Li et al., 1984; Guo and Fan, 1989). The Luanhe river gradually shifted its main course eastwards during the historical period and finally settled down to its present position after the late 19th century (Guo and Fan, 1989). The Suhe River was an isolated river

during the historical period until it was connected to the Luanhe River after artificial channelization for flood mitigation in 1941.

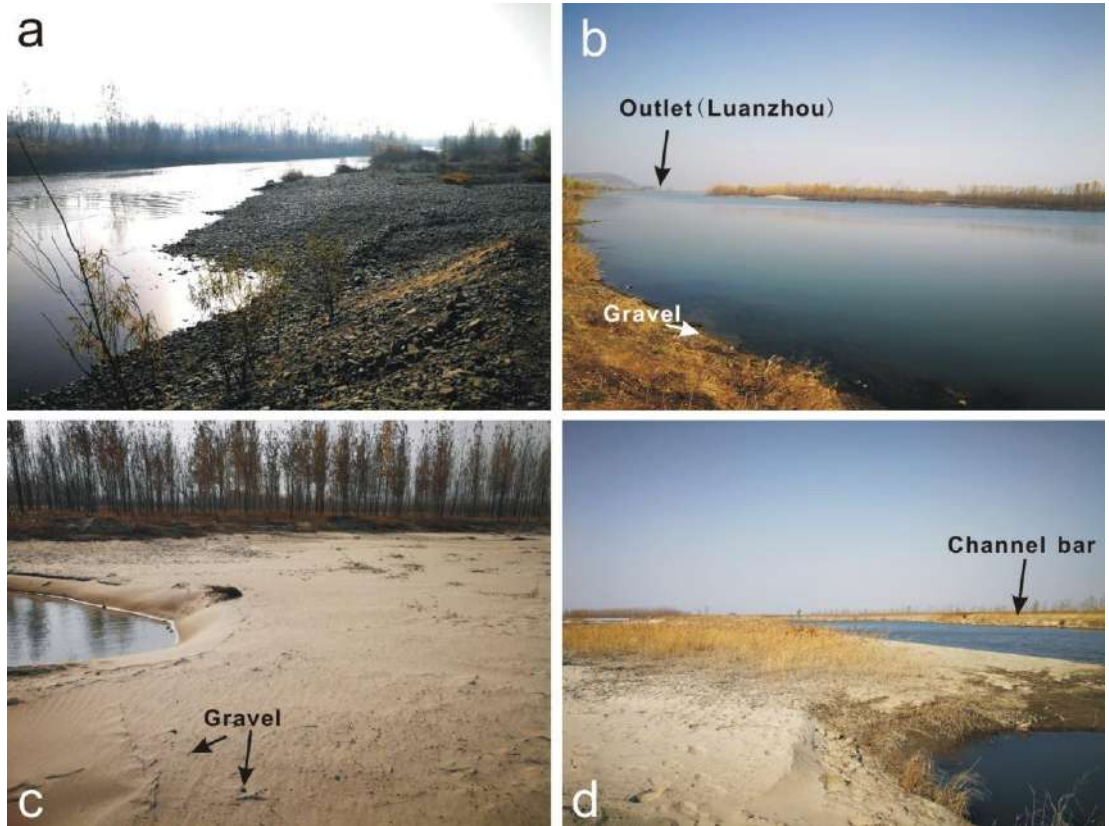


Fig. 2. Landscape of the Lower Luanhe River south of Zhuacun (approximate locations of sites (a) to (d) in Fig.1b). The mean grain size (M_z) of channel-fill sediments is 0.26Φ , 1.95Φ , 2.06Φ , 2.17Φ from site (a) to site (d), respectively.

2.2. Tectonic setting

The Luanhe drainage basin is located at the northeast edge of the China-Korea platform (Liu, 2012). The northern mountain area of the Luanhe drainage basin has kept a steady rise since the Yanshan orogenesis (Old Alpine Stage). Tectonic uplift led to widespread erosion and a generalized stratigraphic gap in this area encompassing the Mesozoic-Cenozoic, except for the intermountain basins (GIDPF et al., 1985). The southern part of the drainage basin (the Bohai Basin), however, continued to

subside, resulting in a several thousand meters thick succession of Cenozoic deposits (GIDPF et al., 1985). Characteristic tectonic uplift in the north and subsidence in the south are the basic structural motifs of the LFD (Liu, 1989).

The LFD is situated at the junction of the Yanshan fold zone and Bohai Basin, where tectonic faults are well developed (Fig. 3). These faults are buried, but they are still active. In 1976, a tremendous and destructive earthquake measuring 7.8 on the Richter scale struck the Tangshan area, leading to hundreds of thousands of deaths and injuries (Guo et al., 1977). The major buried faults in the study area include the Ninghe-Changli Fault (NCF), Lulong-Bogezhuang Fault (LBF), and Luanzhou-Laoting Fault (LLF) (Fig. 3). The NCF, striking in WSW-ENE direction, is located at the northern edge of the Huanghua Depression (HD), which separates the northwest Yanshan fold zone from the Bohai Basin (Liu, 1989; Dong et al., 2010). The LBF, striking in SSW-NNE direction, has a major influence on the flow direction of the lower Luanhe channel north of Luanzhou, and forms the western boundary of the Holocene LFD (Fig. 3; Li et al., 1984; GIDPF et al., 1985). The LLF, which formed during the Paleozoic era and that was recently reactivated, controls the present Luanhe River course with an NNW-SSE direction (Fig. 3; Liu, 1989).

Secondary faults also played an important role in controlling differential subsidence in the study area (Tan and Tian, 2001). These faults separate several sags and saddles within the HD in the coastal area, including Tangshan Saddle, Laoting Sag, Xinanzhuang Saddle, Nanpu Sag and Bogezhuang Saddle (Fig. 3; GIDPF et al., 1985; Tan and Tian, 2001).

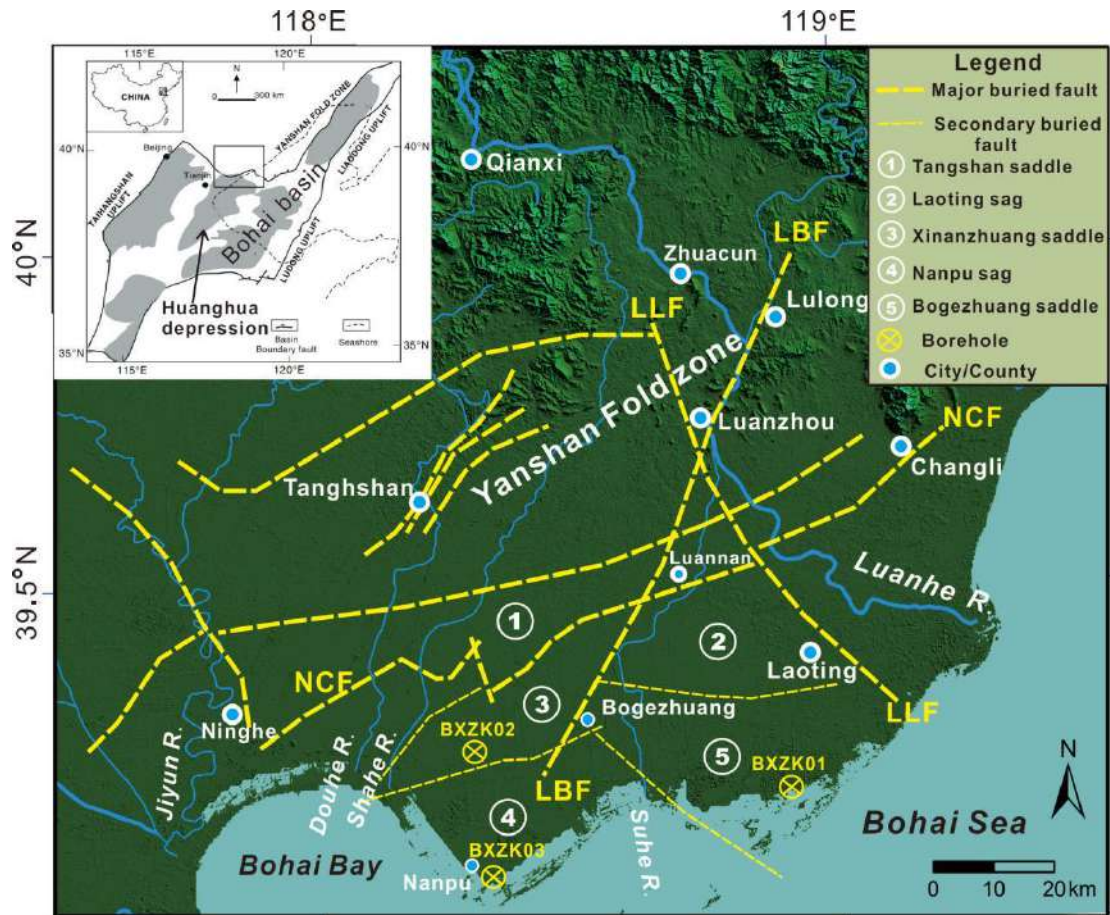


Fig. 3. Tectonic setting and buried faults in the Luanhe Fan-delta area (modified from GIDPF et al., 1985; Dong et al., 2010)

2.3. Climate characteristics

Bounded by the Yanshan Mountains, the lower Luanhe Plain is part of a semi-humid, warm-temperate maritime monsoon climate zone. The northern mountain-hill area has a sub-arid, temperate continental monsoon climate (Liu, 2012). Annual average temperatures range from -1.4°C to 10.6°C in the Luanhe catchment and gradually decrease from south to north (Liu, 2012). Annual precipitations are less than 400 mm in the upstream region (Mongolia Plateau), whereas they average 450~800 mm and ~600 mm in the middle (Yanshan Mountains) and lower (Luanhe

River Plain) areas, respectively (Wang et al., 1990).

Overall, climate in the study area is cold and dry in the winter and hot and rainy in the summer (Liu, 2012). The natural vegetation herein consists of oak forests and psammophytic steppe (Meng et al., 1995). Paleoclimate has changed dramatically in this area since the Late Pleistocene. A preliminary pollen study of a 185 m-long core from the modern Luanhe Delta revealed the paleoclimate evolution of the LLP during the late Quaternary (Jin, 1984). Pollen assemblages, vegetation characteristics and related paleoclimates are shown in Table 1.

Table 1 Paleoclimate changes in the Lower Luanhe Plain during the late Quaternary (modified from Jin, 1984)

Period	Pollen assemblage	Vegetation characteristics	Paleoclimate
Late Holocene (2500 a BP~ present)	<i>Chenopodiaceae-Artemisia</i>	mixed broadleaf-conifer forest (pine and oak) to psammophytic steppe	temperate, semi-humid
Late Middle Holocene (5500~ 2500 a BP)	<i>Pinus-Quercus-Chenopodiaceae</i>	mixed broadleaf-conifer forest (pine and oak)	temperate, slightly arid
Early Middle Holocene (7500~5500 a BP)	<i>Quercus-Pinus-Artemisia-Chenopodiaceae</i>	mixed broadleaf-conifer forest (containing minor evergreen broad leaf)	temperate-warm, humid
Early Holocene (11000~ 7500 a BP)	<i>Pinus-Quercus-Artemisia</i>	mixed broadleaf-conifer forest (pine) to steppe	temperate-cool, slightly arid
MIS2 (24000~11000 a BP)	<i>Artemisia-Bryophyta-Picea</i>	dark coniferous forest (spruce) to steppe	cold, arid
MIS3(60000~24000 a BP)	<i>Quercus-Pinus-Chenopodiaceae</i>	mixed broadleaf-conifer forest (oak) to steppe	temperate, humid
MIS4(80000~60000 a BP)	<i>Bryophyta-Artemisia-Picea</i>	dark coniferous forest to steppe	cold, arid
MIS5(>80000 a BP)	<i>Quercus-Pinus-Artemisia-Chenopodiaceae</i>	mixed broadleaf-conifer forest (pine and oak) to steppe	temperate, humid

2.4. The Luanhe alluvial fan

The lower Luanhe River flows through the Yanshan Fold zone and forms the Luanhe alluvial fan in front of the Yanshan Mountains. Three distinct alluvial fans fed by the Luanhe River have developed since the Early Pleistocene (Fig. 4; Gao, 1985; Guo and Fan, 1989). The oldest fan had its apex in Fengrun, was approximately 3000 km² wide and had a diameter of about 70 km (Guo and Fan, 1989). The upper part of this alluvial fan is still in front of the fold zone, whereas its middle and lower portions have been modified by fluvial and marine processes (Gao, 1985). The apex of the second alluvial fan is located at Xixiakou and the alluvial-fan boundary may reach the Shahe River in the west and the Changli area in the east, with an approximate area of 4000 km² (Gao, 1985; Mo, 1987; Guo and Fan, 1989). The youngest alluvial fan has an area of 1500 km² with its apex in Luanzhou and overlies the second one in the LLP (Fig. 4). From a geomorphic perspective, the youngest alluvial fan can be easily examined, as its peripheral elevations are lower than older deposits in the east and west due to the differential subsidence caused by tectonic faults in this area (see Fig. 3). Average elevation differences are 7–8 m in the eastern side and 2–3 m in the western side, with a more obvious trend toward the northern apex (Luanzhou) (Mo, 1987).

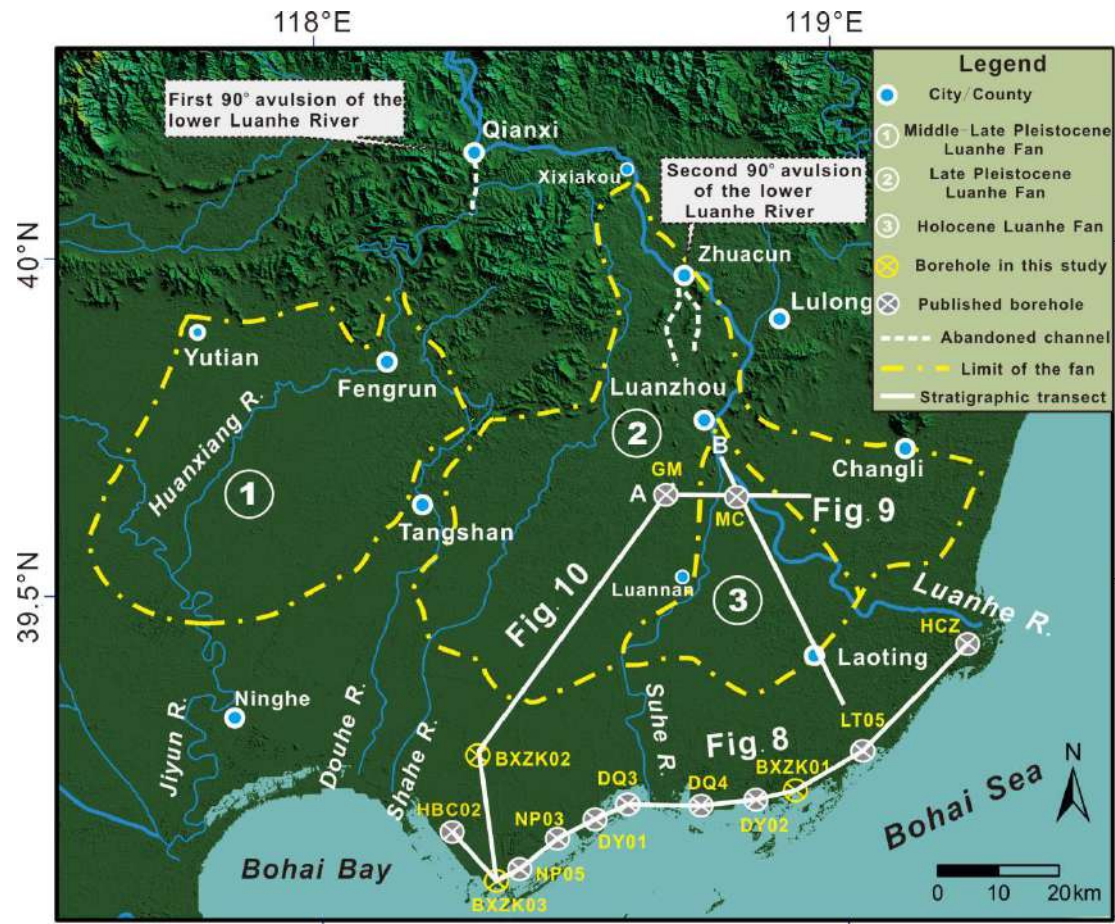


Fig.4 Distribution of three distinct Luanhe alluvial fan systems and stratigraphic profiles across the LFD (modified from Gao, 1985)

3. Methods and materials

Three cores (BXZK01–BXZK03), 90 mm in diameter, were collected from the LLP by rotary drilling in 2016. Their coordinates, elevations and lengths are summarized in Table 2. The mean coring recovery rate of these 3 cores is ~90%. The lithology of each core, as well as sediment color, composition, structure, bedding, fossils, bioturbation, and contacts were examined to identify depositional environments.

227

Table 2 General information about the 3 boreholes drilled in the LFD

Core	Location		Elevation (m)*	Depth (m)	recovery rate
	Latitude	Longitude			
BXZK01	39°11'27.31"E	118°52'24.54"N	1.45	30.6	88.30%
BXZK02	39°17'24.04"E	118°19'35.93"N	1.59	27.3	93.30%
BXZK03	39°02'00.54"E	118°18'38.46"N	3.19	31.52	89.90%

228 *Core elevations are relative to 1956 Yellow Sea height datum of China

229

230 About 320 samples were collected from cores BXZK01–BXZK03 for grain size
231 analysis. The average sampling interval was ~ 0.2 m, with a higher resolution (~0.1 m)
232 where differences in sediment texture were observed. The weight of each sample was
233 about 10 g. Grain size, except for gravel and very coarse sand, was determined using a
234 Mastersizer-2000 laser particle size analyzer, after pre-treating with 10% H₂O₂ and
235 0.10 N HCl to remove organic matter and biogenic carbonates. Twenty-two coarse
236 samples were implemented by the standard sieving methods after pre-treating with
237 distilled water and 0.5 mol.dm⁻³ (NaPO₃)₆ and sorting out the fine particles (<63μm)
238 for drying and weighing. Coarse particles (>63μm) were sifted with a series of
239 selected sieves with opening dimensional interval of ~0.71 mm (0.5Φ) and a pan,
240 fitted into a sieve shaker for 15 minutes. The different size fractions were weighed on
241 an electronic balance with an instrument accuracy of 0.001g and calculated as mass
242 percent in each sample. The remaining 38 samples were processed by combining
243 laser-measurement and sieving methods together. The range of particle sizes was
244 0.02–4000 μm; standard deviations were <1% of the mean values; the reproducibility
245 (φ50) was also <1%. Grain-size classification was based on the Krumbein phi (Φ)
246 scale ([Krumbein and Sloss, 1963](#)). Size parameters in most samples were calculated

247 based on the methods of [Folk and Ward \(1957\)](#), while gravel samples were processed
248 by the GRADISTAT Version 6.0 (see [Blott and Pye, 2008](#)).

249 A total of 14 samples were analyzed for ^{14}C dating with an accelerator mass
250 spectrometer (AMS) (Beta Analytic, Miami). The samples included mainly mollusk
251 shells, organic matter, and plant fragments. Age determinations were based on a Libby
252 half-life of 5568 yr. Radiocarbon ages were corrected for the regional marine
253 reservoir effect ($\Delta R = -139 \pm 59$ a), a regional average determined for the Bohai Sea
254 by [Southon et al. \(2002\)](#) and calibrated using Calib Rev. 7.02 with one standard
255 deviation (1σ) uncertainty ([Reimer et al., 2013](#)).

256 Nine samples for optically stimulated luminescence (OSL) dating were collected
257 in the silty-sandy sections under relatively steady depositional conditions. Each
258 sample was sealed into two black opaque cartridges, 6 cm in height and 3.5 cm in
259 diameter, at a dim environment. All samples were kept in shockproof and lightproof
260 bags and finally examined in the Inspection & Test Center of Marine Geology,
261 Ministry of Natural Resources of China, using the method by [Murray and Wintle](#)
262 [\(2000\)](#).

263 A sum of 135 foraminiferal samples was collected from cores BXZK2 and
264 BXZK03. Average sampling density was ~0.3 m in silty and muddy layers, whereas
265 the sampling interval increased to an average of ~1 m in sandy beds. All samples were
266 dried at 40 °C in an oven, weighed at about 50 g per sample, and washed over a
267 63- μm sieve. After drying, foraminifera were concentrated and separated using the
268 CCl_4 flotation method ([Wang et al., 1985](#)). Sample subdivision was carried out when

the foraminiferal abundance of a sample was very high. A representative number of more than 200 individuals was commonly obtained for each assemblage. Otherwise, all available tests were picked and identified under a Zeiss optical stereoscope. The “foraminiferal abundance” parameter in this study is the number of foraminifera per 50 grams of dry sediment. The “simple diversity” is the number of foraminiferal species in each sample.

4. Results

4.1. OSL and radiocarbon dates

[Table 3](#) summarizes 9 OSL ages that were obtained from 3 boreholes in the LFD. In addition, 14 radiocarbon dates are listed in [Table 4](#).

Table 3 OSL dating results of 9 samples from the LFD

Core	Sample	Depth (m)	Lab No.	U ($\mu\text{g/g}$)	Th ($\mu\text{g/g}$)	K (%)	Mass water content(%)	Dose rate (Gy)	Age (Ka)	Deviation (Ka)
BXZK01	B1S-1	15	2017A059	0.6	3.09	2.12	7.93	58.7	20.9	± 2.1
	B1S-2	21.1	2017A060	0.68	3.49	1.88	6.84	61.7	23.5	± 2.4
	B1S-3	25.74	2017A061	0.91	5.17	2.42	14.21	240.5	70.4	± 7.0
BXZK02	B2S-1	10.06	2017A062	1.32	6.52	2.12	16.58	61.5	18.1	± 1.8
	B2S-2	13.1	2017A063	1.15	4.27	2.4	12.19	110.1	32.4	± 3.2
	B2S-3	18.4	2017A064	0.87	4.64	2.03	8.19	274.2	92	± 9.2
	B2S-4	27.1	2017A065	1.17	6.06	2.34	10.53	>375.0	>105.6	/
BXZK03	B3S-1	14.1	2017A066	0.76	3.89	2.47	15.76	17.9	5.5	± 0.6
	B3S-2	28.4	2017A067	1.22	6.96	2.4	14.2	82	22.2	± 2.2

4.2. Sedimentary facies in cores BXZK01-03

Table 4 Radiocarbon dating results of 14 samples from the LFD

Core	Sample	Depth(m)	Beta no.	Materials	Quality of the dating material	$\delta^{13}\text{C}$ (per mil)	Conventional age (a BP)	Calendar ages (cal a BP)	
								Intercept	Range(1 σ)
BXZK01	BXZK01S5	3.09	472294	<i>Batillaria cumingi</i>	intact gastropod with clear ornamentations	0.5	2020 \pm 30	1795	1718~1864
	BXZK01S1	5.1	461591	<i>Meretrix</i> sp.	shell fragment with slight abrasion	-0.3	3180 \pm 30	3215	3147~3311
	BXZK01S4	7.67	470398	<i>Umbonium thomasi</i>	gastropod fragment with clear ornamentations	1.1	3580 \pm 30	3695	3609~3776
	BXZK01S2	9.95	461592	<i>Potamocorbula ustulata</i>	single valve shell with slight abrasion	-0.2	4780 \pm 30	5305	5248~5414
BXZK02	BXZK02S1	2.13	461594	plant materials	rotted plant fragments	-25.2	107.5 \pm 0.4 pMC	post AD 1950	
	BXZK02S2	5.93	461595	oyster fragments	shell fragments with clear ornamentations	-2.5	5420 \pm 30	5995	5910~6064
	BXZK02S3	7.53	461596	plant materials	rotted plant fragments	-26	7000 \pm 30	7840	7794~7920
	BXZK02S4	24.7	461597	oyster fragments	single valve shell with slight abrasion	-4.7	>43500		
	BXZK02S5	25.53	461598	<i>Arca subcrenata</i>	single valve shell with clear ornamentations	-1.8	>43500		
	BXZK02S6	26.84	461599	shell fragments	shell fragments with clear ornamentations	-4.3	>43500		
BXZK03	BXZK03S1	5.24	461600	organic sediment	bulk organic sediment	-20.7	770 \pm 30	695	675~725
	BXZK03S2	6.85	461601	plant materials	rotted plant fragments	-27.6	3190 \pm 30	3415	3384~3446
	BXZK03S3	24	461602	<i>Talonostrea talonostrea</i>	single valve shell with clear ornamentations	0.4	6120 \pm 30	6675	6604~6751
	BXZK03S4	27.2	461603	<i>Talonostrea talonostrea</i>	single valve shell with clear ornamentations	-1.5	6050 \pm 30	6630	6544~6713

Based on the analysis of lithological and sedimentary characteristics and fossil content from cores BXZK01–03, seven sedimentary facies were identified. They are summarized as follows.

4.2.1. River channel

Depth: Core BXZK01, 29.34–30.6 m, 12.7–25.8 m; Core BXZK02, 17.1–23.2 m, 13–14.8 m, 7.5–10.2 m.

This facies is dominated by yellowish gray to light gray medium–fine sand, gravel sand, and gray coarse silt, with an overall fining-upward trend (Fig. 5a, 6). It has a mean grain size (M_z) of 2.31–5.44 Φ with a fine sand proportion between 30% and 80%, locally as high as 90%. Sorting is moderate to good, with standard deviation (SD) between 0.8 and 2.06 Φ . In particular, mean grain size increases to 1.34–3.07 Φ at 21.3–12.7 m depth in core BXZK01, where average gravel content is 0.5–3 % and the highest values is 10%. Gravels range between 1 and 4 cm in diameter (Fig. 5a).

Black organic mottles and calcareous concretions were occasionally found in some layers. Neither marine shell fragments nor microfossils were found. Freshwater gastropods, such as *Gyraulus albus*, were locally observed. This facies generally has sharp or erosional lower boundary with the underlying depositional units (Fig. 5b).

Thick sand bodies with lower erosional boundary, an overall fining-upward trend, and the occurrence of the terrestrial snail shells are characteristic features of fluvial-channel deposits, possibly laterally accreting riverine systems (Galloway and Hobday, 1983; Miall, 1992; Hori et al., 2001). The overall fining-upward trend is

interpreted to reflect gradual lateral channel shifting (Miall, 1992). The sharp upper boundary indicates sudden abandonment of the river channel (e.g. Amorosi et al., 2008).

Six OSL ages from this facies association range from 92 ± 9 ka BP to 18.1 ± 1.8 ka BP, and at least two fining-upward cycles were observed in cores BXZK01 and BXZK02 (Fig. 6). This implies that this facies was deposited during a long period of time, including multiple cycles of fluvial activity during the Late Pleistocene.

4.2.2. Floodplain

Depth: Core BXZK02, 10.2–13 m, 14.84–17.1 m, 23.2–23.8 m; Core BXZK03, 27.37–31.52 m

This facies consists of gray to dark gray silty clay and silt, locally interbedded with sandy silt layers (Fig. 5b, 5c). The mean grain size of this facies ranges between 4.78Φ and 8.41Φ with poor to very poor sorting (SD: 1.54–2.39). The silt content is 60–70 % with clay 25–35 % and sand <10 %. It displays bioturbation, and also contains plant materials, iron-manganese oxides and calcareous concretions (Fig. 5b). Freshwater gastropods are common in local layers, including *Parafossarulus striatulus* and *Gyraulus albus*. No marine microfossils were found in this facies.

The occurrence of terrestrial mollusks and abundant plant material indicate a terrestrial environment (Galloway and Hobday, 1983). Scattered iron-manganese nodules and calcareous concretions are good indicators of pedogenic processes in a subaerial environment (e.g. Tanabe et al., 2006; Liu et al., 2016). This fine-grained

and poorly sorted depositional unit, thus, is interpreted as formed in a floodplain environment (Miall, 1992). An OSL date from this facies around 22000 a BP in core BXZK03 implies that flood basin development pre-dates the Holocene marine transgression.

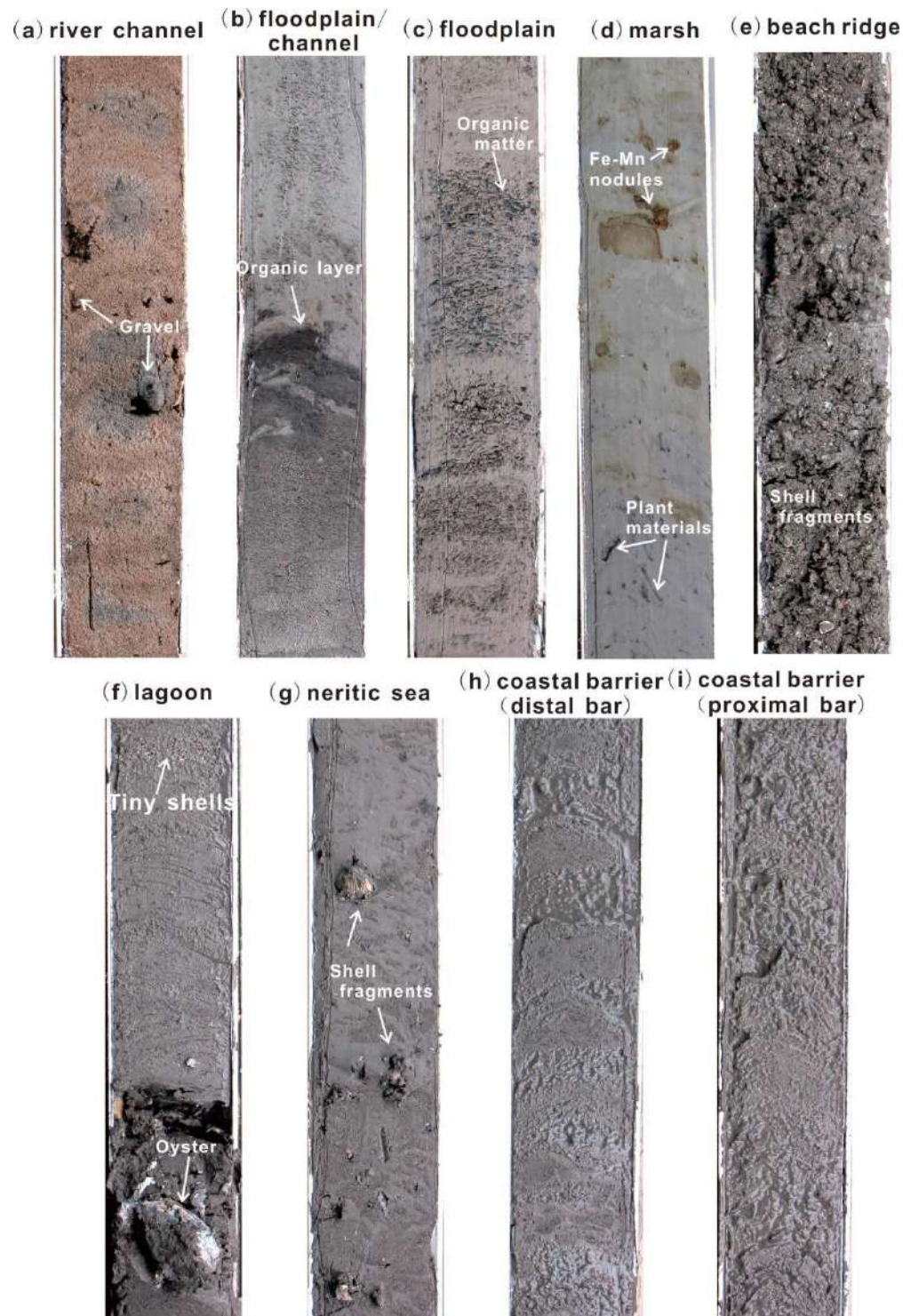


Fig. 5. Representative photographs of sedimentary facies in the LFD

(a) river channel (depth 20.2–20.6 m) in core BXZK01; (b) floodplain and channel (depth 7.3–7.7m) in core BXZK02; (c) floodplain (depth 16.7–17.1m) in core BXZK02; (d) marsh (depth 28.1–28.5 m) in core BXZK01; (e) beach ridge (depth 26.5–26.9m) in core BXZK03; (f) lagoon (depth 5.6–6.0 m) in core BXZK02; (g) neritic sea (depth 24.1–24.5 m) in core BXZK03; (h) coastal barrier (distal bar) (depth 16.2–16.6 m) in core BXZK03; (i) coastal barrier (proximal bar) (depth 12.1–12.5 m) in core BXZK03. All column lengths are 40 cm.

4.2.3. Marsh

Depth: Core BXZK01, 25.8–29.34 m; BXZK02, 6.4–7.5 m

This facies is dominated by greenish to dark gray silty clay and clayey silt (Fig. 5d). The mean grain size (M_z) ranges between 7.02 Φ and 7.81 Φ (standard deviations: 1.25–1.89 Φ), indicating poor sorting. The silt content is 50–60 %, with clay 30–40 % and sand <5 % (Fig. 6). This facies displays horizontal bedding and bioturbation, and also contains organic layers, abundant plant material, scattered iron-manganese nodules and freshwater gastropods, including *Radix* sp. and *Gyraulus albus* (Fig. 5d).

Compared to the floodplain mud, this facies association exhibits a higher proportion of clay and contains lower amounts of silt and sand. The dark gray and greenish color is consistent with a quiescent and submerged depositional environment. Abundant plant material and organic layers are commonly found in marsh or vegetated floodplain (Hori et al., 2004). Given its stratigraphic position atop river channel facies and a lack of marine microfossils (see Fig. 6), this depositional unit can be interpreted as a freshwater marsh formed after abrupt channel abandonment (Galloway and Hobday, 1983).

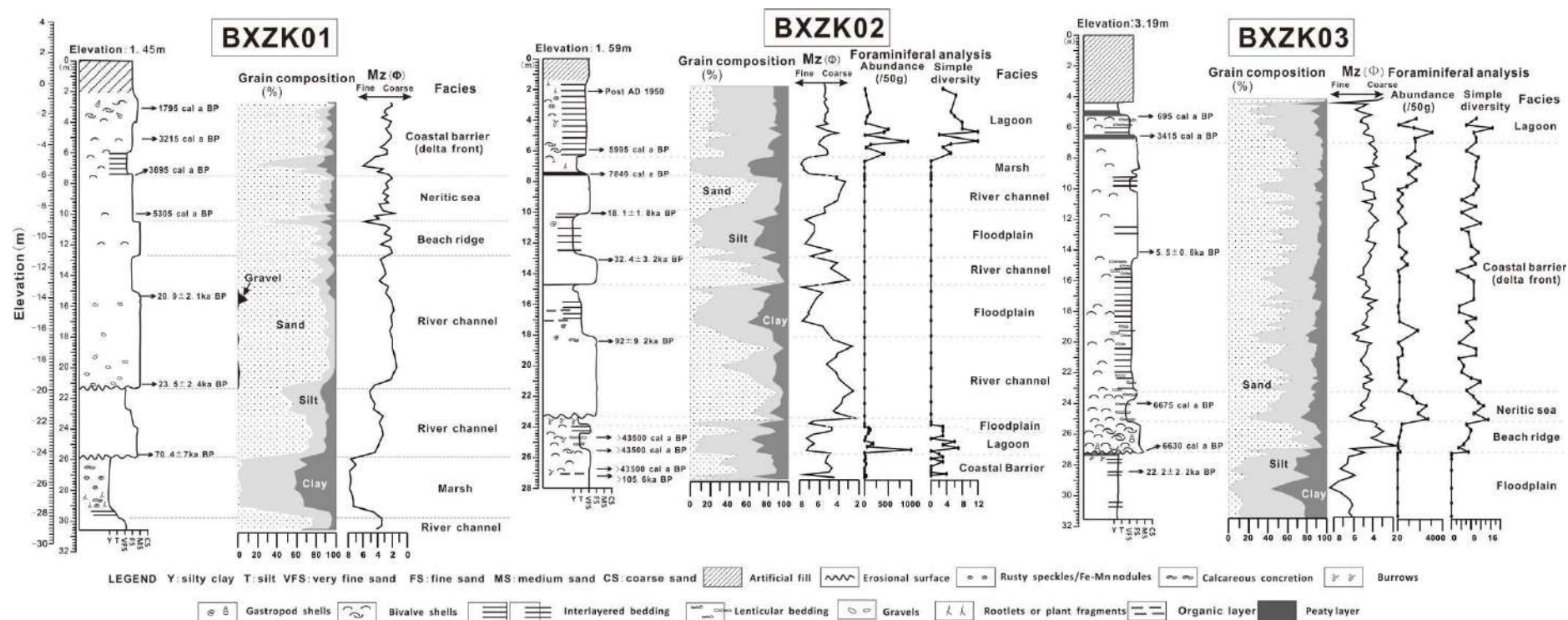


Fig. 6 Stratigraphic logs of cores BXZK01–03 with facies interpretation

4.2.4. Beach ridge

Depth: Core BXZK01, 10.4–12.7 m; BXZK03, 25.3–27.37 m

This unit is dominated by yellowish gray to gray fine and medium sand. It has a mean grain size (M_z) of 1.74–4.54 Φ , with a sand content 60–80 %, silt 15–25% and clay <8% (Fig. 6). Sorting is moderate to good. Lack of sedimentary structures characterizes this unit. Marine mollusk shells are commonly abundant, up to 50% of sediment composition, particularly in core BXZK03 (Fig. 5e), which includes *Talonostrea talonostrea*, *Arca subcrenata*, *Potamocorbula laevis*, *Pelecypora trigona*, *Mitrella bella* and many oyster fragments. In core BXZK03, the average foraminiferal abundance and simple diversity are ~198 and 6, respectively (Fig. 6). The euryhaline *Pararotalia inermis* (average percentage: 24.7 %), *Ammonia beccarii* vars. (22.8%), *Ammonia aomoriensis* (10.1%), are the dominant foraminiferal species (Fig. 7).

Relatively well-sorted coarse sediment rich in marine fossils is characteristic of a high-energy hydrodynamic environment, e.g. foreshore to lower shoreface (Clifton, 2006). Lack of sedimentary structures may reflect poor preservation in core. In some instances, the presence of abundant mollusks in structureless units may reflect rapid deposition from highly concentrated flows during storms (Li et al., 1992; Prager and Halley, 1999) or fossil concentration in a highly reworked deposit. The foraminiferal assemblage, especially the high dominance of *Pararotalia inermis*, indicates a supratidal to intertidal environment (Payros et al., 2000; Wang et al., 2007a). This unit, thus, is interpreted to represent a beach ridge formed by waves during storms or extreme high tides.

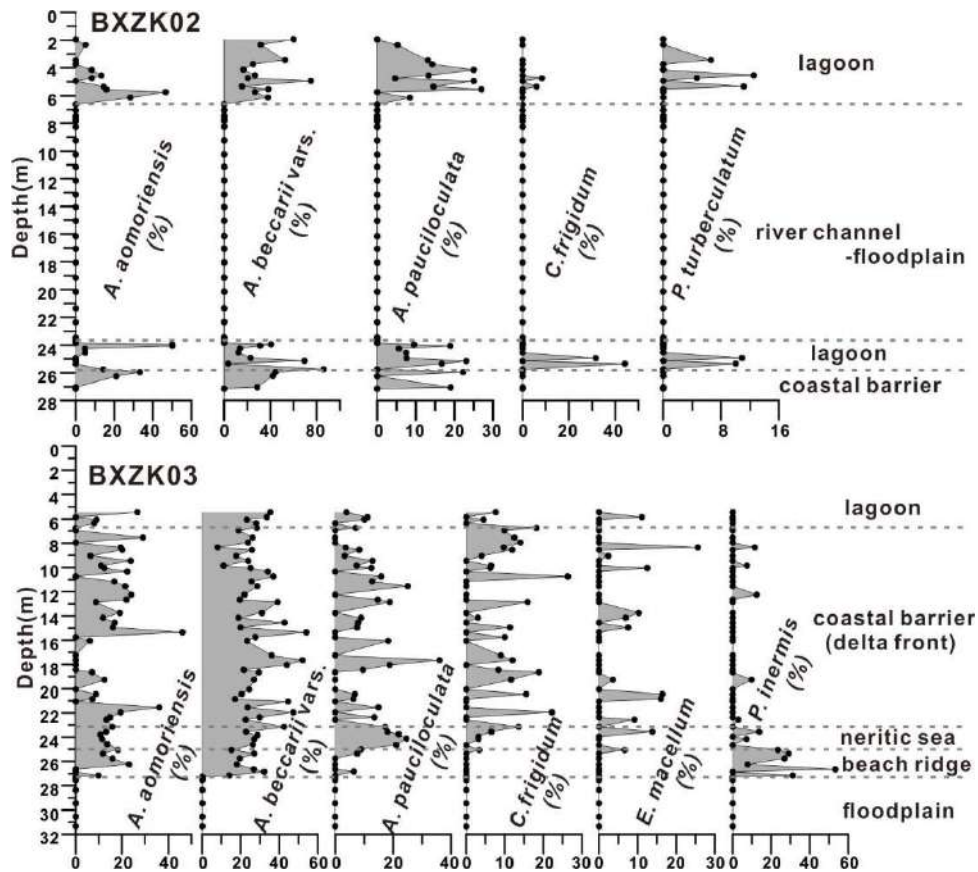


Fig.7. Dominant foraminiferal assemblages in cores BXZK02 and BXZK03

4.2.5. Lagoon

Depth: Core BXZK02, 1.4–6.4 m, 23.8–25.4 m; BXZK03, 4.37–7.0 m

This facies is mainly composed of gray to dark gray coarse silt alternating with gray silty clay (Fig. 5f). The mean grain size ranges from 3.99 Φ to 6.21 Φ , with standard deviation from 1.28 Φ to 2.77 Φ , which indicates poor sorting. The silt content is 50–70 %, with clay 10–20 % and sand 10–20 % (Fig. 6). Brackish water mollusk shells are commonly encountered, including *Crassostrea ariakensis*, *Crassostrea* sp., along with abundant oyster fragments (Fig. 5f). Peat layers and tiny marine shells or fragments are also typically encountered, including *Potamocorbula laevis*, *Umbonium thomasi*, and *Macra veneriformis*. The average abundance and

simple diversity in core BXZK02 are 221 and 7, respectively (Fig. 6). Foraminiferal species are dominated by *A. beccarii* vars. (average percentage: 35.1%) and *A. aomoriensis* (12.4%), whereas relatively stenohaline species *Ammonia pauciloculata* and *Protelphidium turberculatum* exhibit average values of just 13.3% and 5.3%, respectively (Fig. 7). These stenohaline foraminifers are typically distributed from the prodelta to neritic environments off the Yellow River and Yangtze River estuary (Cheng and Xue, 1997; Li and Wang, 1998).

The rhythmical alternation of silt-clay layers in this facies is similar to the characteristic lithology of tidal flat deposits. However, brackish-dominated macrofaunal and microfossil assemblages and the small size of marine fossils indicates a high-salinity, barred marine environment (see in Zinke et al., 2005; Como and Magni, 2009). This facies is interpreted to have formed in a lagoon environment under obvious tidal influence. According to changes in foraminiferal abundance and diversity and concentration of relatively stenohaline species, this unit can also be representative of an open sea (bay) environment (Figs. 6, 7). AMS¹⁴C dates from the lower part of this facies association indicate 5995 cal a BP and 3415 cal a BP (cores BXZK02 and BXZK03, respectively), suggesting that this facies developed in back-barrier position after the maximum marine transgression, following the progradation of coastal barriers or delta systems during the Holocene (Li et al., 1982, 1983; Li and Wang, 1991). In this respect, it can be regarded as a delta plain deposit.

4.2.6. Neritic sea (shallow-marine) and prodelta

Depth: Core BXZK02, 24.4–25.4 m; BXZK03, 23.2–25.3 m

This facies association is dominated by dark gray clayey silt and clayey silt, locally interbedded with gray coarse silt and fine sand lenses (Fig. 5g). It has a mean grain size (M_z) of 6.36–7.31 Φ , with a silt content >55%, clay 10–30% and sand 5–25% (Fig. 6). Sorting is poor to very poor. Bioturbation is very common. Marine mollusk shells are abundant, including *Arca subcrenata*, *Macra veneriformis*, *Potamocorbula laevis*, *Talonostrea talonostrea*, and *Anomia* sp. The average foraminiferal abundance of this facies has the highest value (~1470) of the whole succession in BXZK03. The average value of simple diversity is also the highest, up to 12, in this facies association. The dominant foraminiferal species are *A. beccarii* vars. (average percentage: 22.4%), *A. pauciloculata* (20.7%), *A. aomoriensis* (13.4%), and *Criboelphidium frigidum* (8.2%).

The abundance of marine shells, high concentrations of relatively stenohaline species, and the high degree of bioturbation coupled with a predominantly fine-grained sediment indicate a low-energy and habitable shallow-marine (neritic) environment (see He et al., 2018, 2019). This facies association developed around 5300 cal a BP and 6600 cal a BP in cores BXZK01 and BXZK03, respectively, marking a deepening trend relative to the underlying beach ridge deposits (Fig. 6). Lower bioturbation and a lower fossil abundance in the upper part of the unit likely indicates the onset of a prodelta environment.

4.2.7. Coastal barrier (delta front)

Depth: Core BXZK01, 2.6–7.5 m; BXZK01, 25.4–27.3 m; BXZK03, 7.0–23.8 m

This facies can be subdivided into two parts. The lower part is composed of gray clayey silt interbedded with light gray fine sand and silt (Fig. 5h), containing *Macraa veneriformis*, *Potamocorbula laevis*, *Talonostrea talonostrea*, *Mitrella bella*. The mean grain size ranges from 3.57 Φ to 6.97 Φ , with standard deviation from 1.17 Φ to 2.65 Φ , indicating moderate to poor sorting. The silt content is 30–60 %, with clay 10–20 % and sand 30–50 % (Fig. 6). Lenticular bedding and bioturbation are common. The upper part is dominated by well sorted, light gray to brownish gray fine–medium sand and coarse silt (Fig. 5i). It has a mean grain size (M_z) of 2.75–5.17 Φ , with a sand content 50–70 %, silt 10–30 % and clay <10 % (Fig. 6). Shell fragments of mollusks, such as *Umbonium thomasi*, *Potamocorbula laevis*, *Macraa veneriformis*, *Batillaria cumingi* are commonly found. The average benthic foraminiferal abundance is ~585, and simple diversity reaches ~9 in core BXZK03 (Fig. 6). The dominant foraminifera species are *A. beccarii* vars. (average percentage: 28.7%), *A. aomoriensis* (13.7%), *A. pauciloculata* (7.8%), and *Criboelphidium frigidum* (6.6%) (Fig. 7).

Well-sorted sand in the upper part of this facies association, with fragments of marine shells and the near absence of bioturbation are typical features of the delta front, reflecting high-energy conditions and high sediment accumulation rates (e.g. Abraham et al., 2008; Liu et al., 2009). Silt-sand alternations in the lower part of this facies association are inferred to reflect the prodelta-delta front transition. Considering its occurrence atop shelf deposits and below lagoon clays, this facies

association is likely to represent a coastal barrier, which is the dominant feature of a delta front in a wave-dominated delta (Galloway and Hobday, 1983). A few AMS ^{14}C dates from this facies fall between 3695 and 1795 cal a BP in core BXZK02, whereas AMS ^{14}C and OSL dating indicate an age between 6675 and 3415 cal a BP in core BXZK03 (Fig. 6). The AMS ^{14}C data of this facies are beyond the limits of radiocarbon dating (> 43500 a BP) and older than 105 ka BP of an OSL data in core BXZK02 (Fig. 6), revealing the deposition may be older than MIS 4, probably a MIS 5 marine sedimentation.

5. Discussion

5.1. Sedimentary architecture of the LFD since the Late Pleistocene

Due to the complex stratigraphic architecture of the LFD, the study area was subdivided into two parts, namely the LLP (lower part) and the Luanhe alluvial fan (upper part). The sedimentary architecture of the LFD was synthesized and modeled, as follows.

5.1.1. Late Pleistocene to Holocene sequence stratigraphy of the LLP

To reconstruct the Late-Pleistocene-Holocene stratigraphic architecture of the LLP, well-documented cores (e.g. DQ3, DQ4) and relatively less-studied geotechnical boreholes (e.g. cores HBC02, LT05) were collected from previous and recent studies (Peng et al., 1981; Xu et al., 2020). Combined with detailed core analysis from this

study (Section 4.2), a stratigraphic transect along the present coastline was reconstructed (Fig. 8). The analysis of the stacking patterns of facies framed in a well-constrained chronologic framework enabled a detailed sequence-stratigraphic interpretation for this along-strike profile.

From base to top, river-channel and floodplain deposits of Late Pleistocene age form the lowstand systems tract (LST in Fig. 8). A 3-4 m thick unit dated between about 9.5 and 8.5 ka BP in cores DQ3, DQ4, and DY02, made up of non-marine deposits with an abundance of organic-rich material, is interpreted as a laterally discontinuous transgressive deposit, probably formed in a swampy environment (Fig. 8) and typically marking the onset of the Holocene transgression in onshore position (Amorosi et al., 2017). This unit was not encountered in core BXZK03, where the transgressive surface (TS) records, instead, a significant hiatus and unconformable separates lowstand alluvial deposits from the overlying, littoral to shallow-marine transgressive systems tract (TST). At this location, TST is ~3–5 m thick and includes transgressive coastal barrier, beach-ridge and shallow-marine (neritic) deposits with a characteristic deepening-upward trend above the TS (Fig. 8) that reflects an overall retrogradational pattern. A relatively thick and compound sediment body, ~8–10 m thick, in the middle part of the transect (Fig. 8) is interpreted as a transgressive coastal barrier-lagoon systems formed following the rapid Early Holocene sea-level rise (Xu et al., 2020).

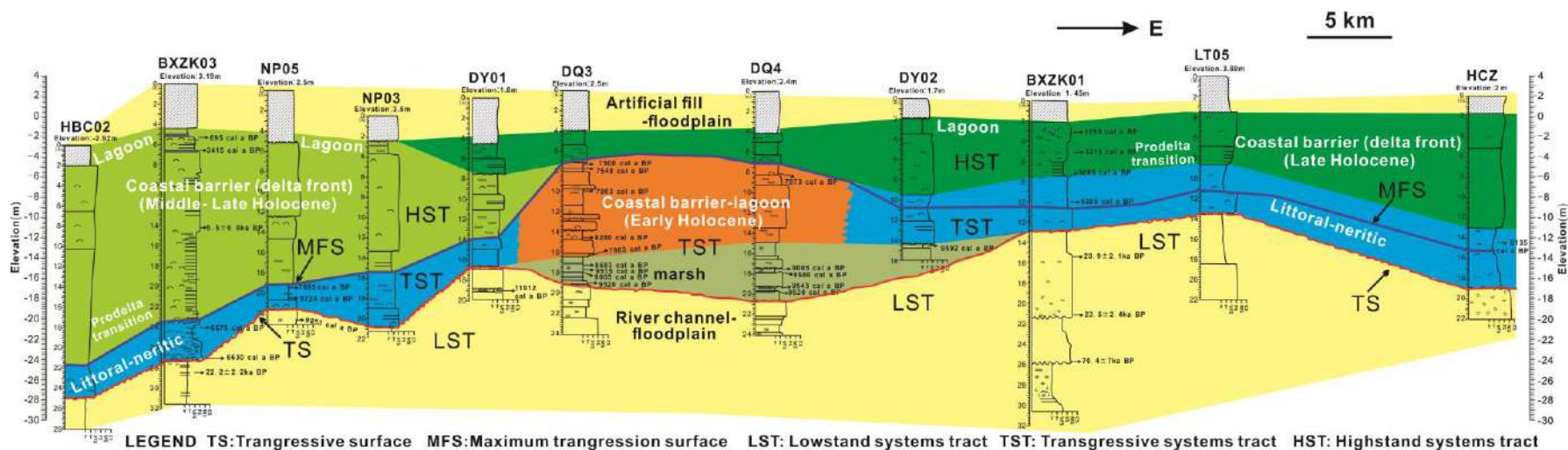


Fig. 8 Stratigraphic transect along the present coastline of the Lower Luanhe Plain

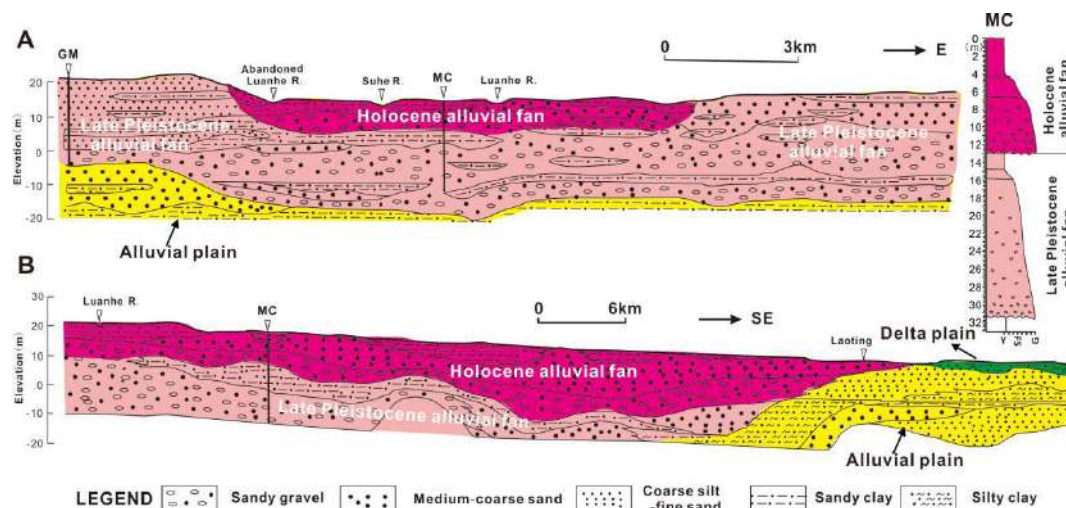


Fig.9. Stratigraphic transects across the Luanhe Fan-delta and log of core MC (after [Li et al., 1984](#); [Mo, 1987](#)). (a) Transversal cross-section in the upper part of LFD, south of Luanzhou. Holocene alluvial fan deposits probably filled an incision into underlying Late Pleistocene alluvial fan deposits. (b) Longitudinal cross-section along LFD. Stratigraphic relations between Holocene alluvial and deltaic deposits are unclear.

Above the maximum flooding surface (MFS), transgressive littoral and shallow-marine deposits are replaced by prograding deltaic units, including prodelta, delta front and delta plain facies that formed in response to the deceleration of sea-level rise (highstand systems tract-HST). Radiocarbon and OSL ages allow the clear separation of distinct phases of coastal barrier development in the different parts of the transect ([Fig. 8](#)). Middle-Late Holocene deposits in the west and Late Holocene coastal facies in the east suggest episodes of delta lobe switching within HST that probably occurred in response to river avulsion and whose location was likely controlled by the presence of the Early Holocene coastal system. Lagoons in a delta plain environment formed due to local compaction following delta lobe abandonment ([Li et al., 1983](#)).

5.1.2. Late Pleistocene to Holocene stratigraphic architecture of the Luanhe alluvial fan

In general, the Luanhe alluvial fan can be considered a “wet” alluvial fan ([GIDPF et al., 1985](#)). Its average gradient is low, between 0.1‰ and 0.88‰ ([GIDPF et al., 1985](#)). These characteristics are similar to the typical “wet” alluvial fans dominated by fluvial processes, showing an upward-fining sequence from gravel sand to sandy silt upwards, such as in the Kosi fan of India ([Agarwal and Bhoj, 1992](#);

Singh et al., 1993; Chakraborty et al., 2010), but distinct from the arid-region, debris-flow dominated alluvial fans that commonly have smaller areas, with high gradients at angles of 1 to 8 degrees (Wasson, 1977; Blair and McPherson, 1994; Nava-Sanchez et al., 1995).

Previous studies have tried to depict the stratigraphic architecture of the Luanhe alluvial fan, based upon the analysis of cores and stratigraphic transects (Li et al., 1984; Mo, 1987). Core data, however, were limited to the inner part of the system (see cores GM and MC in Fig. 4). Two upward-fining cycles, typical of fluvial-channel sequences, can be observed in borehole MC (Fig. 9). Although chronologic constraints are lacking, these cycles can be inferred to represent two phases of alluvial fan development, one of Late Pleistocene age and the other assigned to the Holocene, according to pollen analysis (Li et al., 1984). Other cores, however, basically exhibit a single upward-fining sequence, which may indicate a continuous alluvial-fan environment since the Late Pleistocene. Alluvial stratigraphy (Fig. 9a) was reconstructed with a higher level of detail than the alluvial to deltaic transition in the Laoting area, which remained virtually unexplored (Fig. 9b).

5.1.3. A summary model of the Luanhe fan-delta since the Late Pleistocene

Using stratigraphic transects (Figs. 8, 9) and several well-documented boreholes (such as core BXZK03), detailed stratigraphic relations at the fluvial-marine transition were examined to provide a sequence-stratigraphic interpretation for the northern

Bohai Bay area (Fig. 10).

Under lowstand conditions (LST), the entire study area was characterized by sedimentation in non-marine environments: amalgamated alluvial fan bodies in proximal position show transition at distal locations to alluvial plain (fluvial-channel and floodplain) deposits of Late Pleistocene (Fig. 10b). A transgressive barrier-lagoon system (TST) developed in the coastal area when sea level rose rapidly during the Early Holocene (Fig. 8).

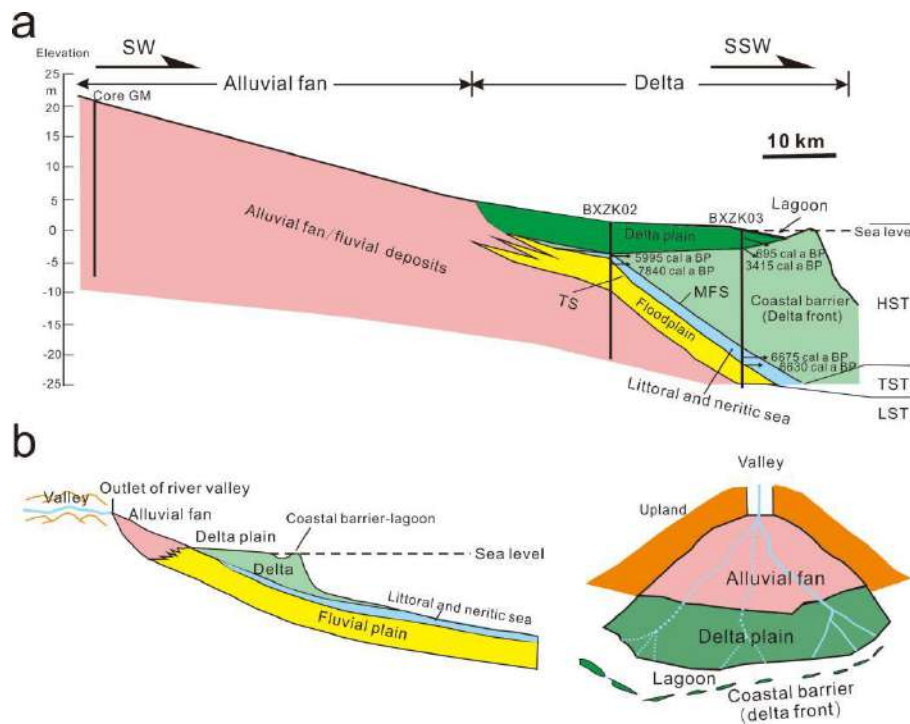


Fig.10. Facies architecture (a) and sequence-stratigraphic interpretation (b) of the Luanhe Fan-delta system (LFD)

A progradational stacking pattern of prodelta, delta front (coastal barrier) and delta plain facies reflects, instead, the seaward migration of the coastline during the following sea-level highstand (HST in Figs. 8, 10). At the same time, a narrower and thinner Holocene alluvial fan system developed on top of older, Late Pleistocene

gravels south of Luanzhou, forming a thick, compound alluvial-fan deposit. The line of maximum transgression is considered in this study as the boundary between alluvial-fan and deltaic depositional systems in the LFD (see Fig. 9).

5.2. Age of Holocene deltaic sedimentation in the LFD

Previous studies have shown that the Holocene LFD distributed approximately in the eastern coastal plain, between the Suhe River and the present Luanhe River as a triangle shaped system with its northern apex located at Luanzhou (Fig. 4). This hypothesis was supported by the presence of two buried active faults with a characteristic X-shaped geometry in planar view (Fig. 3; Li et al, 1984; Guo and Fan, 1989). However, the detailed stratigraphic analysis of core BXZK03 around Nanpu reveals that a Holocene delta system was active in the western coastal plain, as documented by a 17 m-thick succession of coastal barrier (delta-front) deposits between 6600 cal a BP and 3500 cal a BP (Figs. 1b, 6). Consistent with this interpretation, the sedimentologic analysis of core BXZK02, in a relatively landward position, shows the development of coeval delta plain (lagoon) deposits.

Dozens of cores from the Caofeidian Harbour to the Nanpu coastal plain, though lacking detailed facies analysis, revealed the presence of Holocene coastal to shallow-marine deposits (Li and Wang, 1983; Wang, 2000; Wang et al., 2007b; Hu et al., 2017; Xu et al., 2020). According to the isopach of such marine facies in this study (Fig. 11a), the Holocene nearshore successions in the western coastal plain are

up to 30 m thick and are commonly thicker than those in the eastern coastal plain, where maximum values are around 15 m (Fig. 11a). The proximity of these boreholes to core BXZK03 strongly suggests that these marine deposits may also reflect deltaic sedimentation (Fig. 8). As a result, the Luanhe delta plain was not restricted to the area between the Suhe River and the present Luanhe River mouth, but developed also in the west, between the Douhe River and the Suhe River.

Previous research on offshore sandy barriers and subaqueous sand sheets along the Luanhe coastal zone has suggested that the Luanhe subaqueous delta might have existed in the west (Li et al., 1982, 1983; Wang et al., 2013; Xue, 2016). Recent analysis of seismic profiles in the offshore along the Caofeidian Harbour to Nanpu also revealed sedimentary structures of delta progradation in this area (Figs. 11b, 11c; Liu et al., 2019). All of this evidence bolsters our opinion that the Luanhe deltaic system also distributed in the area between the Douhe River and the Suhe River, being supplied from the ancient Luanhe River flowing across this area.

Having barely no reliable chronologic constraints from other boreholes, we took the western deltaic area as a whole delta lobe between the Douhe River and Suhe River. According to data from core BXZK03 (Fig. 6), this western lobe was active until 3500 cal a BP at least, probably initiating when sea level reached a relatively stable position after 7000 cal a BP in Bohai Bay (Liu et al., 2004; Xue, 2014; Tian et al., 2016).

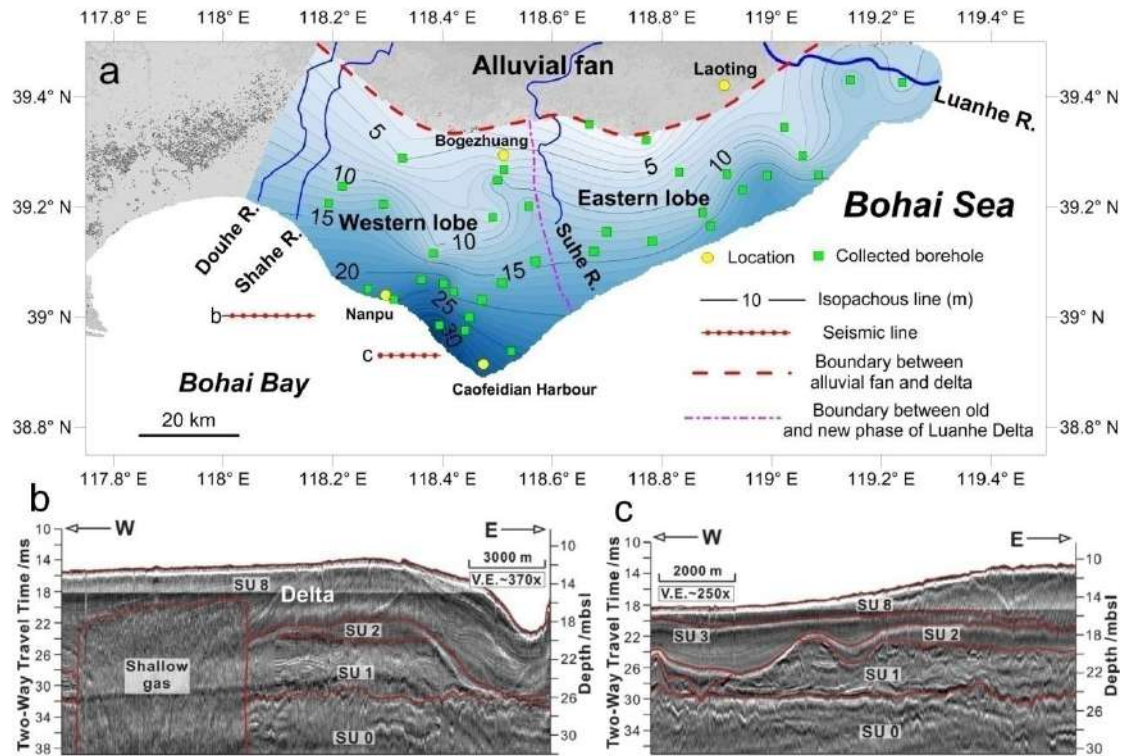


Fig.11. Isopach map (a) and seismic profiles (b, c) of Holocene marine deposits in the northern Bohai coast
(seismic profiles and their interpretations (SU0, 1, 2, 3, 8) modified from [Liu et al., 2019](#))

Although [Li et al. \(1984\)](#) first outlined and distinguished the eastern Holocene Luanhe Delta from the LFD, the delta still has an ambiguous temporal distribution. The lower Luanhe River course shifted to its present position in the early 20th century ([Li et al., 1984](#)). This implies that the modern Luanhe River Delta was active only in the last ~100 years ([Liu, 1989](#)). Radiocarbon dating of several buried peat layers from abandoned fluvial deposits close to Luannan, providing an age range between 2170 ± 150 a BP and 3140 ± 95 a BP ([Peng et al., 1981](#)), indicate that the Luanhe River flowed through the eastern LLP earlier than 3300 cal a BP. Condensed oyster-rich layers have been documented from the Laoting area at 2.5 m depth, with a few radiocarbon dates younger than 3700 ± 80 a BP near the landward limit of the Holocene marine transgression ([Peng et al., 1981](#)). This is probably an indirect

evidence that no significant sediment flux from the ancient Luanhe River discharged in this area before 3800 cal a BP.

Our results from core BXZK01 using an interpolation method reveal that deltaic sedimentation in this area took place after 3700 cal a BP and ended around 1000 cal a BP (Fig. 6). A stranded 33 m-length merchant ship of the Liao Dynasty (825-1043 a BP) was excavated in 1977 near core BXZK01 (Gao, 1981), indicating that the shoreline was close to the position of core BXZK01 around 1000 cal a BP. As no other boreholes with accurate dating have been documented from the eastern LLP, based on data from core BXZK01 we conclude that the eastern delta lobe started to develop after ~3700 cal a BP (Fig. 6), and that it is still active.

Using borehole data from Xu et al. (2020), a new transect along the present coastline was reconstructed in this work (see Fig. 8). This transect strongly suggests that two phases of deltaic progradation took place around 7000–3500 cal a BP (western delta lobe) and 3700 cal a BP– present (eastern delta lobe). The Early Holocene transgressive coastal barrier-lagoon recovered in the middle part of the coastal area might have played a role in separating the two phases of delta lobe development.

5.3. River avulsions and sedimentary evolution of the LFD since the late Quaternary

Based upon our research findings and previous studies, three phases of sedimentary evolution for the LFD are synthesized and reconstructed since the late

Quaternary, as follows.

5.2.1. Phase I: Pleistocene (> 15000 cal a BP)

Previous studies have shown that during the Early Pleistocene the main Luanhe River course passed by the present Huanxiang River course and flowed south to Fengrun in the western part of the northern Bohai coastal plain (NBCP) (Figs. 4, 12a; Gao, 1987). At that time, it formed the huge Luanhe alluvial fan, with an estimated area of 3000 km². Its apex was located in Fengrun, and its eastern edge could have been as far as the Douhe River area (Fig. 4, 12a; Guo and Fan, 1989). Another alluvial fan with its apex in Luanzhou might have been built during this period by the Qinglong River (Figs. 9, 12a).

The Luanhe alluvial fan was active for most of the Pleistocene, until a dramatic 90-degree diversion in Qianxi sequestered a significant part of the sediments delivered to this area (GIDPF et al., 1985; Gao, 1987). Although no direct dating allows assessing the age of this river avulsion accurately, it has been considered to have occurred earlier than 13000 a BP, based on the ¹⁴C dating of ancient tree trunks from the terrace (T2) of the ancient Luanhe River (Gao, 1987). The Luanhe River likely had simultaneously two distinct downstream directions, south and east of Qianxi for a short period around 13000 a BP. Another ¹⁴C date from an ancient tree trunk in alluvial deposits south of Xixiakou yielded an age of 15245±230 a BP, revealing that shifting of the main river course in Qianxi probably took place earlier than 15000 a BP (Peng et al., 1981; Gao, 1987).

661

662 *5.2.2. Phase 2: Latest Pleistocene–Early Holocene (15000–7000 cal a BP)*

663 Following the abrupt avulsion in Qianxi, a new alluvial fan was formed by the
664 Luanhe River, with its apex in Xixiakou (Figs. 4, 12b; Gao, 1987; Guo and Fan, 1989;
665 Wang et al., 2007b). Several abandoned channel segments are still visible on the
666 alluvial fan at the landscape scale, indicating the frequent shifts of the lower Luanhe
667 river course in this area (Fig. 1b).

668 The alluvial fan, with an estimated area of 4000 km², spread from the Shahe
669 River in the west to the Changli area in the east (Figs. 4, 12b; Gao, 1985; Mo, 1987;
670 Guo and Fan, 1989). Its axial diameter was as long as 100 km (Guo and Fan, 1989).
671 During phases 1 and 2, an alluvial plain distributed in front of the alluvial fan (Figs.
672 12a, b).

673 The Early Holocene marine transgression approached the present coastline around
674 9000 cal a BP, as inferred by age dating reported by Xu et al. (2020). The ancient
675 Luanhe River possibly emptied into the Bohai Bay in the middle part of the LLP,
676 approximately around the present Suhe River. With the punctuated sea-level rise
677 during 9.5–7 cal ka BP, a compound coastal barrier-lagoon system emerged under
678 transgressive conditions.

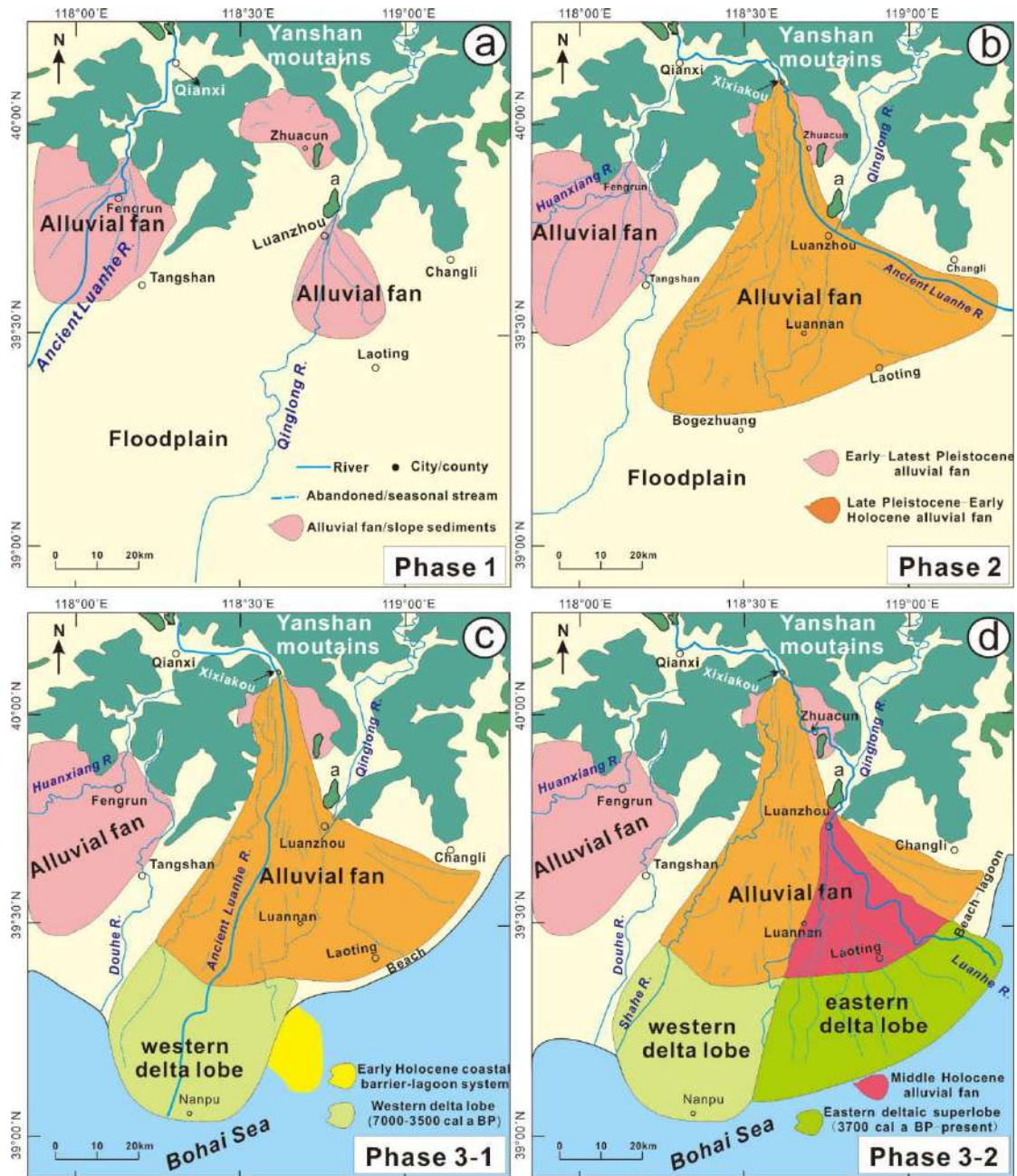


Fig.12. Sedimentary evolution of the Luanhe Fan-delta since the Late Quaternary (alluvial fan modified after Gao, 1985; Liu, 1989)

(a) phase 1: Early-Late Pleistocene; (b) phase 2: Late Pleistocene (c) phase 3-1: 7000–3500 cal a BP; (d) phase 3-2: 3700 cal a BP– present;

5.2.3. Phase 3: 7000 cal a BP~ Present

Alluvial sedimentation was terminated by the Early Holocene marine transgression. The transgressive coastal to shallow-marine depositional setting,

testified by a veneer of littoral and shallow-marine facies associations, developed in the study area around 7000 cal a BP (Figs. 8, 10). When the Holocene marine transgression approached its maximum in the Bohai Sea around 7000 cal a BP (Xue, 2009, 2014), highstand prograding deltas accumulated in the study area on top of thin retrograding systems, forming the Holocene LFD of the modern coastal plain (Figs. 10, 12c). From 7000 cal a BP to 3500 cal a BP, LFD was focused between the present Douhe River and Suhe River (Fig. 12c).

A second nearly 90-degree diversion then took place in Zhuacun (Fig. 12d), resulting in remarkable paleoenvironmental changes in the LFD evolution (Fig. 4; Gao, 1987; Wang et al., 2007b; Xue, 2016). The Luanhe River turned eastwards and captured the Qinglong River north of Luanzhou, forming a new LFD with its apex in Luanzhou (see Figs. 1b, 4). The Holocene alluvial fan, distributing between the Suhe River and present Luanhe River, had an area of 1500 km², and fluvial channels entrenched onto the Pleistocene alluvial fan (Fig. 4, 5; Guo and Fan, 1989). Meanwhile, deltaic sedimentation extended in front of the Holocene alluvial fan, forming the distal part of the new LFD (Fig. 12d).

As for the Holocene avulsion, no precise dating constrains the time in which the Luanhe River shifted its course at Zhuacun. Previous studies have hypothesized a latest Pleistocene to Early-Middle Holocene age on the basis of a few ¹⁴C dates of cores south of Luanzhou (Peng et al., 1981; Li et al., 1984; Gao, 1987). However, as the older delta system was formed between 7000–3500 cal a BP and the new delta lobe initiated after 3700 cal a BP (Fig. 6; Fig. 12d), we suggest that the Holocene

course shifting at Zhuacun might have occurred around 3600 ± 100 cal a BP.

5.4. Controlling factors on the development of the LFD

Tectonic, climatic and base-level changes are widely accepted as important controlling factors in the development of alluvial fans (Bull, 1991; Singh et al., 2001; Harvey et al., 2002; Benvenuti, 2003; Kumar et al., 2007; Clevis et al., 2010). The same factors may also have played a role in the development and evolution of the Luanhe fan-delta in the lower Luanhe Plain.

Tectonically-controlled river avulsions have largely been documented in rivers that flow across tectonically-active regions, such as the Rhine-Meuse system (Berendsen and Stouthamer, 2000), the Tisza River (Timár et al., 2005) and the Pearl River (Yao et al., 2013). This commonly implies fan-delta abandonment and building of a new system, such as in the case of the Godavari delta (Rao et al., 2015). Additionally, tectonic activity can also govern sedimentary processes in foreland lacustrine or marine basins (Dorsey et al., 1995; Benvenuti, 2003), which may largely impact the distal portion of fan-deltas. As already stated in section 5.3, two nearly 90-degree diversions of the lower Luanhe River occurred at the edge of the Yanshan fold zone in the latest Pleistocene-Holocene, leading to remarkable paleoenvironmental changes in the sedimentary evolution of the LFD (Figs. 4, 12). Given the very high degree of seismicity in the study area, it is likely that these two river avulsions were closely related to the eastward tilting movements that controlled

differential uplift and subsidence between the western side and eastern side of the LLP since the late Quaternary (Liu, 1989; Wang et al., 2007b). These eastward tilting movements could also account for the constant river shifting of the Luanhe River mouth toward northeast, with nearly 70 km displacement since the late 13th century in this area (Fig.1b). Differential uplift/subsidence might also have impacted the stratigraphic architecture of the LFD since the Late Pleistocene. Cores BXZK01 and BXZK02 are located in the Boge Zhuang Saddle and Xinzhuang Saddle respectively, whereas core BXZK03 is situated in the Nanpu sag (Fig. 3). Stratigraphic correlation of these three cores reveals remarkable differences that might reflect tectonic control: for example, relatively old (MIS 3 to MIS 5) deposits were observed around 25 m depth in the area of cores BXZK01 and BXZK02, but significantly younger deposits were encountered at the same depth in the area of core BXZK03 (Fig. 6). Similarly, the thickness of Holocene deltaic deposits is >18 m in core BXZK03, whereas it is < 6 m from the two cores recovered in the saddles (Fig. 6). Our data from the northern coastal area of the Bohai Sea (Bay) are consistent with previous studies from the western and southern coastal plain, which hypothesized an important role of neotectonics in shaping the late Quaternary stratigraphic architecture (see Fig. 8 in Liu et al., 2016).

Previous studies revealed that paleoclimate changed dramatically since the Late Pleistocene in this area (Table. 1; Jin, 1984). Climate amelioration or deterioration generally imply changes in the vegetation coverage, leading to the mobilization or stabilization of the landscape in the drainage basin and, eventually, to dramatic

changes in sediment load (Syvitski, 2002; West et al., 2005; Liu et al., 2008; Lu et al., 2013). This is more and more emphasized as a critical factor in controlling the aggradation or entrenchment in alluvial fans (Pope et al., 2016; Chen et al., 2016; Terrizzano et al., 2017). As stated above, the LFD is a typically stream-dominated fan-delta where flows the perennial Luanhe River with a predominantly mountain-hill drainage (Fig. 1a). During glacial periods (such as MIS4 and MIS2), the vegetation coverage may have decreased in the study area due to the dry and cold climate, resulting in severe soil and water loss in the Luanhe catchment. The high sediment discharge enhanced the development of the Luanhe Fan and its area reached the maximum extent (approximately 4000 km²) close to the Last Glacial Maximum (Gao, 1985; Guo and Fan, 1989). Gao (1985) estimated that the average accretion rate of the Luanhe alluvial fan was as high as 7 mm/a during the last glacial period. With the subsequent climatic amelioration during the interglacial period, the Luanhe River saw an increase in water discharge, but still was characterized by low sediment loads, as a result of the high vegetation coverage. Alluvial fan incision and entrenchment dominated, and the aggradation of the fan during the Holocene was quite smaller (only 0.2-0.7mm/a) than that of the glacial period (Gao, 1985). However, sediment discharge into the Holocene Luanhe Delta gradually increased, similar to other alluvial fans (Meyer et al., 1992). The Holocene Luanhe Delta prograded rapidly and formed two deltaic lobes in the lower part of the LFD since the Middle Holocene. In this regard, the development of the LFD may partly be related to Holocene climate changes in the study area.

Base-level change caused by climate fluctuations or tectonic activity is commonly considered as a critical factor in controlling progradation/aggradation and incision/entrenchment of alluvial fans ([Harvey et al., 1999](#); [Harvey et al., 2002](#); [Robustelli et al., 2005](#); [Kumar et al., 2007](#)) and may exert a significant influence in the proximal parts of fan-delta systems. The whole Luanhe Fan-delta area has been characterized by the regionally Yanshan Mountains uplift and persistent depression of the Bohai basin since the Cenozoic era ([Guo et al., 2007](#); [Li et al., 2010](#)). Previous studies estimated that the uplift rates of the southern Yanshan Mountains in our study area may have been as high as 0.118mm/a ([Wu et al., 2000](#)), whereas subsidence rates in the Bohai Basin ranged between 0.061 mm/a and 0.184 mm/a during the Cenozoic era ([Ren et al., 2008](#)). If base-level changes caused by eustatic fluctuations during the Late Pleistocene are not taken into account, the constant base-level fall can roughly be estimated between 21.3 m and 35.8 m in the LFD since the Late Pleistocene, basically the same thickness of the upper-middle fan zone of the LFD (~30 m) during the same period. This implies that accommodation due to uplift and subsidence could have been sufficient to host the alluvial deposits, which likely hold back the extension of the fan area southwards in the Lower Luanhe Plain in a pristine condition.

Sea level has fluctuated worldwide since the Late Pleistocene, including the Bohai Sea and adjacent seas ([Liu et al., 2004](#); [Xue, 2014](#); [Song et al., 2018](#)). Late Quaternary sea-level fluctuations clearly influenced the stratigraphic architecture in the study area. Coastal and shallow-marine deposits accumulated under transgressive /highstand conditions related to the last and present interglacials (MIS 5 and Holocene,

respectively). On the other hand, fully alluvial sedimentation with no delta development characterized phases of sea-level fall and lowstand related to the intervening glacial periods (MIS 4 to MIS 2). As a result, alluvial-fan systems expanded and retreated, as a function of sea-level fall and subsequent rise. In particular, deltas initiated during periods of sea-level highstand, and then prograded seawards, overlying areas originally occupied by alluvial fans and alluvial plains (Figs. 10b, 12c). Major falls in sea level during glacial periods can greatly increase channel gradient and potentially increase stream power sufficiently to trigger fluvial incision and fan entrenchment (see Waters et al., 2010). This process may decrease when sea level gradually rises during interglacial periods. During the MIS5 and the Holocene, sea level rose up to the present shoreline, as suggested by marine and transitional facies in core BXZK01–03. The difference in relief between the mountain pass and sea level became smaller, inhibiting river channel incision. The Luanhe alluvial fan decreased to a smaller size. During the low sea-level periods, such as MIS2 and MIS4, the Luanhe alluvial fan widely spread across the study area. The transport capacity of the Luanhe River greatly enhanced during these period, because of the high difference in relief relative to the base level. Stream flows and debris flows occurred frequently, resulting in considerably larger alluvial fans (Fig. 12b). Deltas and fluvial plain were replaced by alluvial systems during this period. Thus, eustatic changes might have controlled, in part at least, fan-delta evolution in the distal parts of the system by means of paleoenvironment changes and fluvial hydrodynamics.

6. Conclusions

Based on the comprehensive analysis of three ~30 m-long cores from the Lower Luanhe Plain (LLP), including sedimentary facies, microfossils and integrated AMS¹⁴C and OSL dating, the Late Pleistocene-Holocene stratigraphic architecture of the Luanhe Fan-delta system (LFD) was reconstructed in detail. The LFD evolved from an ancient coastal barrier-lagoon system during MIS5 to river channels, floodplains and marshes between MIS4 and the Early Holocene. Depositional environments rapidly evolved from non-marine to littoral and shallow-marine environment under transgressive conditions since the Early Holocene. Progradation of coastal barrier (delta front) and lagoon (delta plain) systems during the following highstand was influenced by the transgressive antecedent topography. A stratigraphic cross-section parallel to the present coastline, with along-strike orientation, revealed that distinct delta lobes developed lateral to the Early Holocene transgressive coastal barrier-lagoon system. The western delta lobe was active between 7000 cal a BP and 3500 cal a BP, while the eastern one developed after ~3700 cal a BP and is still active at the present.

Three phases of sedimentary evolution in the inner (fluvial) part of LFD were reconstructed in the northern Bohai coastal plain (NBCP). During the Pleistocene, an alluvial fan with an area of ~3000 km² formed with its apex in Fengrun in the western part of the NBCP. During the Latest Pleistocene (~15000 cal a BP), the lower Luanhe River turned eastwards after a dramatic avulsion in Qianxi, and formed a larger alluvial fan (~4000 km² wide) with its apex at Xixiakou in the eastern NBCP. When

sea level reached its highstand position around 7000 cal a BP, progradation of the Luanhe delta took place in front of or partly overlying the distal part of the alluvial fan. Following the eastward shift of the Lower Luanhe River, a second dramatic avulsion at Zhuacun in 3600±100 cal a BP formed a new LFD with its apex in Luanzhou. These two avulsions of the Lower Luanhe River were likely controlled by intense tectonic activity in a region with extremely high seismic risk. Climate changes and base-level changes also played a role in the sedimentary evolution of the LFD since the late Quaternary.

Acknowledgements

This study was jointly funded by the Key Program for International S&T Cooperation Projects of China (Grant No. 2016yfe0109600), China Geological Survey projects (Grant Nos. DD20160144, DD20189503) and the National Natural Science Foundation of China (Grant Nos. 41706057, 41876057). We thank Xianghuai Kong, Hongming Yuan, Guangming Zhao, Guohua Hou, Yanxiang Lei and Ruoshun Guo for their help in the geological survey or in manuscript preparation.

References

- Abraham, B.M.S., Nichol, S.L., Parker, R.J., Gregory, M.R., 2008. Facies depositional setting, mineral maturity and sequence stratigraphy of a Holocene drowned valley, Tamaki Estuary, New Zealand. *Estuar. Coast Shelf Sci.* 79, 133-142.
- Agarwal, R.P., Bhoj, R., 1992. Evolution of Kosi river fan, India: structural implications and geomorphic significance. *Int. J. Remote Sens.* 13, 1891-1901.
- Amorosi, A., Bruno, L., Campo, B., Morelli, A., Rossi, V., Scarponi, D., Wan, H., Bohacs, K.M., Drexler, T.M., 2017. Global sea-level control on local parasequence architecture from the Holocene record of the Po Plain, Italy. *Mar. Petrol. Geol.*, 87, 99-111.
- Amorosi, A., Pavesi, M., Lucchi, M.R., Sarti, G., Piccin, A., 2008. Climatic signature of cyclic fluvial architecture from the Quaternary of the central Po Plain, Italy. *Sediment. Geol.* 209, 58-68.
- Benvenuti, M., 2003. Facies analysis and tectonic significance of lacustrine fan-deltaic successions in the Pliocene-Pleistocene Mugello Basin, Central Italy. *Sediment. Geol.* 157, 197-234.
- Blair, T.C., McPherson, J.G., 1994. Alluvial fans and their natural distinction from rivers based on morphology, hydraulic processes, sedimentary processes, and facies assemblages. *J. Sediment. Res.* 64, 450-489.
- Berendsen, H.J.A., Stouthamer, E., 2000. Late Weichselian and Holocene palaeogeography of the Rhine-Meuse delta, The Netherlands. *Palaeogeogr. Paleoclimatol.* 161, 311-335.
- Blott, S.J., Pye, K., 2008. Particle shape: a review and new methods of characterization and classification. *Sedimentology* 55, 31-63.
- Bull, W.B., 1991. *Geomorphic Responses to Climatic Change*. Oxford University Press, Oxford, 326 pp.
- Chakraborty, T., Kar, R., Ghosh, P., Basu, S., 2010. Kosimegafan: Historical records, geomorphology and the recent avulsion of the Kosi River. *Quatern. Int.* 227, 143-160.
- Chen, L., Steel, R.J., Guo, F., Olariu, C., Gong, C., 2016. Alluvial fan facies of the Yongchong Basin: Implications for tectonic and paleoclimatic changes during Late Cretaceous in SE China. *J. Asian Earth Sci.* 134, 37-54.
- Cheng, G., Xue, C., 1997. *Sedimentary geology of the Yellow River Delta* (in Chinese). Geological publishing house, Beijing, pp. 48-137.
- Clevis, Q., Boer, P.L.D., Nijman, W., 2010. Differentiating the effect of episodic tectonism and eustatic sea-level fluctuations in foreland basins filled by alluvial fans and axial deltaic systems: insights from a three-dimensional stratigraphic forward model. *Sedimentology* 51, 809-835.
- Clifton, H.E., 2006. A reexamination of facies models for clastic shorelines, in: Posamentier, H.W., Walker, R.G. (Eds.), *Facies models revisited*. Society for Sedimentary Geology, Oklahoma, pp. 293-337.
- Coleman, J.M., Wright, L.D., 1975. *Modern River Deltas: Variability of Processes and Sand Bodies*. Houston Geological Society, Houston, pp. 99-149.
- Como, S., Magni, P., 2009. Temporal changes of a macrobenthic assemblage in harsh lagoon sediments. *Estuar. Coast Shelf Sci.* 83, 638-646.
- Dong, Y., Xiao, L., Zhou, H., Wang, C., Zheng, J., Zhang, N., Xia, W., Ma, Q., Du, J., Zhao, Z.,

2010. The Tertiary evolution of the prolific Nanpu Sag of Bohai Bay Basin, China: Constraints from volcanic records and tectono-stratigraphic sequences. *Geol. Soc. Am. Bull.* 122, 609-626.

Dorsey, R.J., Umhoefer, P.J., Renne, P.R., 1995. Rapid subsidence and stacked Gilbert-type fan deltas, Pliocene Loreto basin, Baja California Sur, Mexico. *Sediment. Geol.* 98, 181-204.

Feng, J.L., Zhang, W., 1998. The evolution of the modern Luanhe River delta, north China. *Geomorphology* 25, 269-278.

Folk, R.L., Ward, W.C., 1957. Brazos River bar: a study in the significance of grain size parameters. *J. Sediment. Petrol.* 31, 514-519.

Galloway, W.E., Hobday, D.K., 1983. Terrigenous clastic depositional systems: applications to petroleum, coal, and uranium exploration. Springer, New York, pp. 25-111.

Gao, S., 1981. Facies and sedimentary model of the Luan River Delta (in Chinese with English abstract). *Acta Geogr. Sinica* 36, 303-314.

Gao, S., 1985. Structures and sedimentary environments of the alluvial fan of the Luan River (in Chinese with English abstract). *Geogr. Res.* 4, 54-62.

Gao, S., 1987. Quaternary changes of middle-lower channels of the Luanhe River (in Chinese). *Memo. Geogr.* 18, 52-63.

GIDPF (Geologica Institute of Dagang Petroleum Field), MPEB (Marine Petroleum Exploration Bureau), MGITU (Marine Geology Institute of Tongji University), 1985. Luanhe River alluvial fan-delta sedimentary system (in Chinese). Geological Publishing House, Beijing, 164 pp.

Guo, S., Li, Z., Cheng, S., Chen, X., Chen, X., Yang, Z., Li, R., 1977. Discussion on the regional structural background and the seismogenic model of the Tangshan earthquake (in Chinese with English abstract). *Sci. Geol. Sinica*. 4, 305-321.

Guo, W., Fan, C., 1989. Historical Migration and Hydrological Characteristics of the Lower Luanhe River (in Chinese). *Geogr. Terr. Res.* 5, 45-51.

Guo, X., Shi, X., Qiu, X., Wu, Z., YANG, X., Xiao, S., 2007. Cenozoic subsidence in Bohai Bay Basin: Characteristics and dynamic mechanism (in Chinese with English abstract). *Geotect. Metallog.* 31, 273-280.

Harvey, A.M., Church, M., Hassan, M.A., 2002. The role of base-level change in the dissection of alluvial fans: case studies from Southeast Spain and Nevada. *Geomorphology* 45, 67-87.

Harvey, A.M., Silva, P.G., Mather, A.E., Goy, J.L., Stokes, M., Zazo, C., 1999. The impact of Quaternary sea-level and climatic change on coastal alluvial fans in the Cabo de Gata ranges, southeast Spain. *Geomorphology* 28, 1-22.

He, L., Xue, C., Ye, S., Laws, E.A., Yuan, H., Yang, S., Du, X., 2018. Holocene evolution of the Liaohe Delta, a tide-dominated delta formed by multiple rivers in Northeast China. *J. Asian Earth Sci.* 152, 52-68.

He, L., Xue, C., Ye, S., Amorosi, A., Yuan, H., Yang, S., Laws, E., 2019. New evidence on the spatial-temporal distribution of superlobes in the Yellow River Delta Complex. *Quat. Sci. Rev.* 214, 117-138.

Hori, K., Saito, Y., Zhao, Q., Cheng, X., Wang, P., Sato, Y., Li, C., 2001. Sedimentary facies of the tide-dominated paleo-Changjiang (Yangtze) estuary during the last transgression. *Mar. Geol.* 177, 331-351.

Hori, K., Tanabe, S., Saito, Y., Haruyama, S., Nguyen, V., Kitamura, A., 2004. Delta initiation and

950 Holocene sea-level change: example from the Song Hong (Red River) delta, Vietnam.
 951 Sediment. Geol. 164, 237-249.

952 Hu, G., Zhuang, Z., Yin, P., Zhao, D., Liu, S., Wang, L., 2017. The hole D219 and the Late
 953 Quaternary paleogeographic environments in the northern Bohai Bay, China (in Chinese with
 954 English abstract). Mar. Geol. Front. 33, 16-23.

955 Hwang, I.G., Chough, S.K., Hong, S.W., Choe, M.Y., 1995. Controls and evolution of fan delta
 956 systems in the Miocene Pohang Basin, SE Korea. Sediment. Geol. 98, 147-179.

957 Jia, H., Ji, H., Li, X., Hang, Z., Wang, L., Yan, G., 2016. A retreating fan-delta system in the
 958 Northwestern Junggar Basin, northwestern China—Characteristics, evolution and controlling
 959 factors. J. Asian Earth Sci. 123, 162-177.

960 Jia, H., Ji, H., Wang, L., Yan, G., Li, X., Hang, Z., 2017. Reservoir quality variations within a
 961 conglomeratic fan-delta system in the Mahu sag, northwestern Junggar Basin: Characteristics
 962 and controlling factors. J. Petrol. Sci. Eng. 152, 165-181.

963 Jiang, T., Fang, X., Xu, H., Guo, W., 1986. Analysis of Runoff and Sand Transport in Luanhe
 964 Estuary (in Chinese). J. Oceanogr. Huanghai Bohai Seas 4, 93-106.

965 Jin, X., 1984. The spore-pollen assemblages and the stratigraphy and palaeogeography in western
 966 Bohai Sea since Late Pleistocene (in Chinese with English abstract). Mar. Sci. Bull. 3, 16-24.

967 Kim, J.W., Chough, S.K., 2000. A gravel lobe deposit in the prodelta of the Doumsan fan delta
 968 (Miocene), SE Korea. Sediment. Geol. 130, 183-203.

969 Krumbein, W.C., Sloss, L.L., 1963. Stratigraphy and Sedimentation. Free Man, San Francisco,
 970 401pp.

971 Kumar, R., Suresh, N., Sangode, S.J., Kumaravel, V., 2007. Evolution of the Quaternary alluvial
 972 fan system in the Himalayan foreland basin: Implications for tectonic and climatic
 973 decoupling. Quatern. Int. 159, 6-20.

974 Li, C., Chen, G., Gao, M., Zhuang, Z., 1982. Sedimentation and Development of the
 975 barrier-lagoon systems along the coastal zone of East China (in Chinese with English
 976 abstract). Mar. Geol. Res. 2, 47-56.

977 Li, C., Chen, G., Wang, C., Zhang, Y., 1984. On the Luanhe River alluvial fan-delta complex (in
 978 Chinese with English abstract). Acta Petrol. Sinica 5, 27-36.

979 Li, C., Chen, G., Wang, L., 1983. The abandoned delta of the Luanhe River and the barrier-lagoon
 980 sedimentary systems (in Chinese with English abstract). Acta Sediment. Sinica 1, 61-71.

981 Li, C., Han, C., Wang, P., 1992. Depositional Sequences and Storm Deposition on Low-energy
 982 Coast of China (in Chinese with English abstract). Acta Sediment. Sinica 10, 119-128.

983 Li, C., Li, P., Wang, L., Wang, C., Zhang, Y., 1985. Facies assemblage of present Luanhe Delta (in
 984 Chinese with English abstract). Sci. Geol. Sinica 2, 202-210.

985 Li, C., Wang, P., 1991. Stratigraphy of the Late Quaternary barrier-lagoon depositional systems
 986 along the coast of China. Sediment. Geol. 72, 189-200.

987 Li, C., Wang, P., 1998. Estuarine stratigraphy in the late Quaternary of the Yangtze River (in
 988 Chinese). Science Press, Beijing, pp. 1-222.

989 Li, G., Yin, Y., 2010. Recent geomorphological evolution of downstream channel and delta of
 990 Luanhe River (in Chinese with English abstract). Geogr. Res. 29, 1606-1615.

991 Li, H., Wang, J., 1983. Palaeomagnetic study on drill core from northern Bohai coastal plain (in
 992 Chinese with English abstract). Geochimica 2, 196-204.

993 Li, S., Suo, Y., Dai, L., et al., 2010. Development of the Bohai Bay Basin and destruction of the

994 North China Craton (in Chinese with English abstract). *Earth Sci. Front.* 17, 65-89.

995 Li, Y., Gao, S., An, F., 1982. A preliminary study of the Quaternary marine strata and its
996 paleogeographic significance in the Luanhe Delta region (in Chinese with English abstract).
997 *Ocean. Limn. Sinica* 13, 433-439.

998 Liu, C., Sui, J., Wang, Z.Y., 2008. Sediment load reduction in Chinese rivers. In. *J. Sediment Res.*
999 23, 44-55.

1000 Liu, F., 1989. An analysis of relationship between the development and texural characteristics of
1001 the alluvial fan deltas in the lower reaches of the Luanhe River using remote sensing data (in
1002 Chinese with English abstract). *Coast. Eng.* 8, 44-50.

1003 Liu, J., Saito, Y., Wang, H., Zhou, L., Yang, Z., 2009. Stratigraphic development during the Late
1004 Pleistocene and Holocene offshore of the Yellow River delta, Bohai Sea. *J. Asian Earth Sci.*
1005 36, 318-331.

1006 Liu, J., Wang, H., Wang, F., Qiu, J., Saito, Y., Lu, J., Zhou, L., Xu, G., Du, X., Chen, Q., 2016.
1007 Sedimentary evolution during the last ~ 1.9 Ma near the western margin of the modern
1008 Bohai Sea. *Palaeogeogr. Paleoclimatol.* 451, 84-96.

1009 Liu, J.P., Milliman, J.D., Gao, S., Cheng, P., 2004. Holocene development of the Yellow River's
1010 subaqueous delta, North Yellow Sea. *Mar. Geol.* 209, 45-67.

1011 Liu, S., Feng, A., Liu, C., Zheng, Y., Li, P., Zhang, Z., 2019. Seismic stratigraphy and morphology
1012 of the Holocene progradational system beneath Bohai Bay, Bohai Sea: Lobate evolution of a
1013 multi-sourced subaqueous fluvial deltaic complex. *Mar. Geol.* 409, 31-47.

1014 Liu, Y., 2012. An Analysis of the Hydrology, Geology and Economic Situation of Luanhe River
1015 Basin (in Chinese with English abstract). *J. Hebei Normal Univ. Nat. Sci. Ed.* 32, 24-26.

1016 Lonne, I., Nemec, W., 2010. High-arctic fan delta recording deglaciation and environment
1017 disequilibrium. *Sedimentology* 51, 553-589.

1018 Lopez-Blanco, M., Marzo, M., Burbank, D.W., Verges, J., Roca, E., Anadon, P., Pina, J., Steel,
1019 R.J., 2000. Tectonic and climatic controls on the development of foreland fan deltas;
1020 Montserrat and Sant Llorenç del Munt systems (middle Eocene, Ebro Basin, NE Spain).
1021 *Sediment. Geol.* 138, 17-39.

1022 Lu, X., Ran, L., Liu, S., Jiang, T., Zhang, S., Wang, J., 2013. Sediment loads response to climate
1023 change: A preliminary study of eight large Chinese rivers. In. *J. Sediment Res.* 28, 1-14.

1024 McPherson, J.G., Shanmugam, G., Moiola, R.J., 1988. Fan-deltas and braid deltas: Varieties of
1025 coarse-grained deltas. *Geol. Soc. Am. Bull.* 100, 1308-1310.

1026 Meng, L., Xu, Q., Yue, L., Zhang, D., 1995. Vegetation feature of different depositional facies and
1027 different geomorphological zones on the lower reach of the Luan River (in Chinese with
1028 English abstract). *J. Hebei Acad. Sci.* 5, 20-26.

1029 Meyer, G.A., Wells, S.G., Balling, R.C., Jull, A.J.T., 1992. Response of alluvial systems to fire and
1030 climate change in Yellowstone National Park. *Nature* 357, 147-150.

1031 Miall, A.D., 1992. Alluvial deposits, in: Walker, R.G., James, N.P. (Eds.), *Facies Models: Response*
1032 *to Sea Level Change*. Geological Association of Canada, Waterloo, pp. 119-139.

1033 Mo, Y., 1987. A preliminary study of the lower ancient Luanhe River course (in Chinese). *Memo.*
1034 *Geogr.* 18, 64-73.

1035 Murray, A.S., Wintle, A.G., 2000. Luminescence dating of quartz using an improved single-aliquot
1036 regenerative-dose protocol. *Radiat. Meas.* 32, 57-73.

1037 Nava-Sanchez, E., Cruz-Orozco, R., Gorsline, D.S., 1995. Morphology and sedimentology of two

- contemporary fan deltas on the southeastern Baja California Peninsula, Mexico. *Sediment. Geol.* 98, 45-61.
- Nava-Sanchez, E.H., Gorsline, D.S., Cruz-Orozco, R., Godinez-Orta, L., 1999. The El Coyote fan delta: A wave-dominated example from the Gulf of California, Mexico. *Quatern. Int.* 56, 129-140.
- Orton, G.J., Reading, H.G., 1993. Variability of deltaic processes in terms of sediment supply, with particular emphasis on grain size. *Sedimentology* 40, 475-512.
- Park, M.E., Cho, H., Son, M., Sohn, Y.K., 2013. Depositional processes, paleoflow patterns, and evolution of a Miocene gravelly fan-delta system in SE Korea constrained by anisotropy of magnetic susceptibility analysis of interbedded mudrocks. *Mar. Petrol. Geol.* 48, 206-223.
- Payros, A., Astibia, H., Cearreta, A., Pereda-Suberbiola, X., Murelaga, X., Badiola, A., 2000. The Upper Eocene South Pyrenean Coastal deposits (Liedena sandstone, navarre): Sedimentary facies, benthic foraminifera and avian ichnology. *Facies* 42, 107-131.
- Peng, G., Jiao, W., Li, D., Li, G., 1981. Division and correlation of the Late Quaternary stratigraphy and discussion on the recent tectonic movement in the region of the Luanhe River Delta (in Chinese with English abstract). *Seismol. Geol.* 3, 31-36.
- Pope, R.J.J., Candy, I., Skourtos, E., 2016. A chronology of alluvial fan response to Late Quaternary sea level and climate change, Crete. *Quaternary Res.* 86, 170-183.
- Prager, E.J., Halley, R.B., 1999. The Influence of Seagrass on Shell Layers and Florida Bay Mudbanks. *J. Coastal Res.* 15, 1151-1162.
- Rao, K.N., Saito, Y., Nagakumar, K.C.V., Demudu, G., Rajawat, A.S., Kubo, S., Zhen, L., 2015. Palaeogeography and evolution of the Godavari delta, east coast of India during the Holocene: An example of wave-dominated and fan-delta settings. *Palaeogeogr. Paleoclimatol.* 440, 213-233.
- Reimer, P.J., Bard, E., Bayliss, A., Beck, J.W., Blackwell, P.G., Ramsey, C.B., Buck, C.E., Cheng, H., Edwards, R.L., Friedrich, M., Grootes, P.M., Guilderson, T.P., Haffliger, H., Hajdas, I., Hatté, C., Heaton, T.J., Hoffmann, D.L., Hogg, A.G., Hughen, K.A., Kaiser, K.F., 2013. Intcal 13 and Marine13 Radiocarbon age Calibration curves 0-50,000 years Cal BP. *Radiocarbon* 55, 1869-1874.
- Ren, F., Liu, Z., Qiu, L., Han, L., Zhou, L., 2008. Space-time discrepancy of depressionalevolution in the Bohai Bay Basin during Cenozoic (in Chinese with English abstract). *Chinese J. Geol.* 43, 546-557.
- Robustelli, G., Muto, F., Scarciglia, F., Spina, V., Critelli, S., 2005. Eustatic and tectonic control on Late Quaternary alluvial fans along the Tyrrhenian Sea coast of Calabria (South Italy). *Quat. Sci. Rev.*, 24(18), 2101-2119.
- Rohais, S., Eschard, R., Guillocheau, F., 2008. Depositional model and stratigraphic architecture of rift climax Gilbert-type fan deltas (Gulf of Corinth, Greece). *Sediment. Geol.* 210, 132-145.
- Singh, A.K., Parkash, B., Mohindra, R., Thomas, J.V., Singhvi, A.K., 2001. Quaternary alluvial fan sedimentation in the Dehradun Valley Piggyback Basin, NW Himalaya: tectonic and palaeoclimatic implications. *Basin Res.* 13, 449-471.
- Singh, H., Parkash, B., Gohain, K., 1993. Facies analysis of the Kosimegafan deposits. *Sediment. Geol.* 85, 87-113.
- Song, B., Yi, S., Yu, S.Y., Nahm, W.H., Lee, J.Y., Lim, J., Kim, J.C., Yang, Z., Min, H., Jo, K.N., 2018. Holocene relative sea-level changes inferred from multiple proxies on the west coast of

- South Korea. *Palaeogeogr. Paleocl.* 496, 268–281.
- Southon, J., Kashgarian, M., Fontugne, M., Metivier, B., Yim, W.W.-S., 2002. Marine reservoir corrections for the Indian Ocean and Southeast Asia. *Radiocarbon* 44, 167–180.
- Syvitski, J.P., 2002. Sediment discharge variability in Arctic rivers: implications for a warmer future. *Polar Res.* 21, 323–330.
- Tan, L., Tian, S., 2001. Faulting and volcanism in cenozoic of Nanpu depression (in Chinese with English abstract). *J. Univ. Petrol. China* 25, 1–5.
- Tanabe, S., Saito, Y., Vu, Q.L., Hanebuth, T.J.J., Ngo, Q.L., Kitamura, A., 2006. Holocene evolution of the Song Hong (Red River) delta system, northern Vietnam. *Sediment. Geol.* 187, 29–61.
- Terrizzano, C.M., Morabito, E.G., Christl, M., Likerman, J., Tobal, J., Yamin, M., Zech, R., 2017. Climatic and Tectonic forcing on alluvial fans in the Southern Central Andes. *Quat. Sci. Rev.* 172, 131–141.
- Tian, L.Z., Tao, Y.B., Jiang, X.Y., Chen, Y.S., Shi, P.X., Shang, Z.W., Li, J.F., Wang, F., Wang, H., 2016. Reconstruction of the Holocene relative sea level change for the south coast of Laizhou Bay (in Chinese with English abstract). *Geol. Bull. China* 35, 1679–1691.
- Timár, G., Sümegei, P., Horváth, F., 2005. Late Quaternary dynamics of the Tisza River: Evidence of climatic and tectonic controls. *Tectonophysics* 410, 97–110.
- Wang, P., Min, Q.B., Bian, Y.H., 1985. Distributions of foraminifera and ostracoda in bottom sediments of the northwestern part of the South Huanghai (Yellow) Sea and its geological significance (in Chinese). in: Wang, P. (Ed.), *Marine Micropaleontology of China*. China Ocean Press, Beijing, pp. 93–114.
- Wang, R., Zhang, X., Wang, X., 1990. Analysis of hydrological characteristics of Luanhe River drainage basin (in Chinese). *Hydrology* 3, 51–54.
- Wang, S., Liu, J., Wu, C., Yu, M., 2007a. Foraminifera assemblages and its sediment environment in Qianhu Bay of Zhangpu, Fujian (in Chinese with English abstract). *Journal of Oceanography in Taiwan Strait* 26, 151–156.
- Wang, W., Fu, Y., Li, S., Li, P., 2013. Distribution on surface sediment and sedimentary divisions in the middle part of Bohai Sea (in Chinese with English abstract). *Acta Sediment. Sinica* 31, 478–485.
- Wang, Y., 2000. Restorations of Paleoenvironments in Caofeidian Area since the Last stage of the Late Pleistocene Epoch (in Chinese with English abstract). *J. Oceanogr. Huanghai Bohai Seas* 18, 1–6.
- Wang, Y., Fu, G., Zhang, Y., 2007b. River-sea interactive sedimentation and plain morphological evolution (in Chinese with English abstract). *Quat. Sci.* 27, 674–689.
- Wasson, R.J., 1977. Last-glacial alluvial fan sedimentation in the Lower Derwent Valley, Tasmania. *Sedimentology* 24, 781–799.
- Waters, J.V., Jones, S.J., Armstrong, H.A., 2010. Climatic controls on late Pleistocene alluvial fans, Cyprus. *Geomorphology* 115, 228–251.
- Wei, W., Zhu, X., Tan, M., Guo, D., Hui, S., Zhao, Q., Jiang, F., 2015. Reservoir characteristics and influences on poroperm characteristics of the Lower Cretaceous fan-delta facies in Chagan Depression (in Chinese with English abstract). *Oil Gas Geol.* 36, 447–455.
- West, A.J., Galy, A., Bickle, M., 2005. Tectonic and climatic controls on silicate weathering. *Earth Planet. Sci. Lett.* 235, 211–228.

- 1126 Winsemann, J., Asprien, U., Meyer, T., Schramm, C., 2007. Facies characteristics of Middle
1127 Pleistocene (Saalian) ice-margin subaqueous fan and delta deposits, glacial Lake Leine, NW
1128 Germany. *Sediment. Geol.* 193, 105-129.
- 1129 Wu, Z., Cui, S., Wu, G., Zhu, D., Feng, X., Ma, Y., 2000. Thermochronological analysis on the
1130 uplift process of the Yanshan Mountains (in Chinese with English abstract). *Geol. Rev.* 46,
1131 49-57.
- 1132 Xu, Q., Meng, L., Yuan, G., Teng, F., Xin, H., Sun, X., 2020. Transgressive wave-and
1133 tide-dominated barrier-lagoon system and sea-level rise since 8.2 ka recorded in sediments in
1134 northern Bohai Bay, China. *Geomorphology* 352, 106978.
- 1135 Xue, C., 2009. Historical changes of coastlines on west and south coasts of Bohai Sea since 7000
1136 a B.P. (in Chinese with English abstract). *Sci. Geogr. Sinica* 29, 217-222.
- 1137 Xue, C., 2014. Missing evidence for stepwise postglacial sea level rise and an approach to more
1138 precise determination of former sea levels on East China Sea Shelf. *Mar. Geol.* 348, 52-62.
- 1139 Xue, C., 2016. Extents, type and evolution of Luanhe River Fan-delta system, China (in Chinese
1140 with English abstract). *Mar. Geol. Quat. Geol.* 36, 13-22.
- 1141 Yao, Y., Zhan, W., Liu, Z., Zhang, Z., Zhan, M., Jie, S., 2013. Neotectonics and its Relations to the
1142 Evolution of the Pearl River Delta, Guangdong, China. *J. Coastal Res.* 66, 1-11.
- 1143 Zinke, J., Reijmer, J.J.G., Taviani, M., Dullo, W.C., Thomassin, B., 2005. Facies and faunal
1144 assemblage changes in response to the Holocene transgression in the Lagoon of Mayotte
1145 (Comoro Archipelago, SW Indian Ocean). *Facies* 50, 391-408.

Marine Geology

We the undersigned declare that this manuscript is original, has not been published before and is not currently being considered for publication elsewhere.

We confirm that the manuscript has been read and approved by all named authors and that there are no other persons who satisfied the criteria for authorship but are not listed. No conflict of interest exists in the submission of this manuscript, and manuscript is approved by all authors for publication.

We understand that the Corresponding Author is the sole contact for the Editorial process. He/she is responsible for communicating with the other authors about progress, submissions of revisions and final approval of proofs.

Signed by all authors as follows:

Lei He, Alessandro Amorosi, Siyuan Ye, Chunting Xue, Shixiong Yang